



GR2005-2

# GEOSCIENTIFIC REPORT

## Geology of the Black Island area, Lake Winnipeg, Manitoba (parts of NTS 62P1, 7 and 8)



By  
A.H. Bailes  
and J.A. Percival



---

**Geoscientific Report GR2005-2**

# **Geology of the Black Island area, Lake Winnipeg, Manitoba (parts of NTS 62P1, 7 and 8)**

by A.H. Bailes and J.A. Percival  
Winnipeg, 2005

---

Industry, Economic Development and Mines

Hon. Jim Rondeau  
Minister

Hugh Eliasson  
Deputy Minister

Mineral Resources Division

C.A. Kaszycki  
Assistant Deputy Minister

Manitoba Geological Survey

E.C. Syme  
Director

Every possible effort is made to ensure the accuracy of the information contained in this report, but Manitoba Industry, Economic Development and Mines does not assume any liability for errors that may occur. Source references are included in the report and users should verify critical information.

Any digital data and software accompanying this publication are supplied on the understanding that they are for the sole use of the licensee, and will not be redistributed in any form, in whole or in part, to third parties. Any references to proprietary software in the documentation and/or any use of proprietary data formats in this release do not constitute endorsement by Manitoba Industry, Economic Development and Mines of any manufacturer's product.

When using information from this publication in other publications or presentations, due acknowledgment should be given to the Manitoba Geological Survey. The following reference format is recommended:

Bailes, A.H. and Percival, J.A. 2005: Geology of the Black Island area, Lake Winnipeg, Manitoba (parts of NTS 62P1, 7 and 8); Manitoba Industry, Economic Development and Mines, Manitoba Geological Survey, Geoscientific Report GR2005-2, 33 p.

**NTS grid:** 62P1, 62P7, 62P8

**Keywords:** basalts, Black Island, Black Island assemblage, calc-alkalic composition, economic geology, fuchsite, geochemistry, geochronology, gold ores, island arcs, komatiite, Lake Winnipeg, Lewis-Storey assemblage, lithogeochemistry, Manitoba, Neoproterozoic, North Caribou Terrane, ocean floors, plate tectonics, Rice Lake belt, rifting, Superior Province

**External author addresses:**

J.A. Percival  
Geological Survey of Canada  
615 Booth Street  
Ottawa, ON K1A 0E9  
(613) 995-4723  
E-mail: John.Percival@nrcan-rncan.gc.ca

**Published by:**

Manitoba Industry, Economic Development and Mines  
Manitoba Geological Survey  
360–1395 Ellice Avenue  
Winnipeg, Manitoba  
R3G 3P2 Canada  
Telephone: (800) 223-5215 (General Enquiry)  
(204) 945-4154 (Publication Sales)  
Fax: (204) 945-8427  
E-mail: minesinfo@gov.mb.ca  
Website: <http://www.gov.mb.ca/iedm/mrd/>

**Cover illustration:** View of Lake Winnipeg north of Black Island.

## Abstract

The Black Island area is located at the boundary between a Mesoarchean craton, the ca. 3.0 Ga North Caribou Terrane, and Neoarchean 2.72–2.71 Ga volcanic and sedimentary rocks of the Uchi Subprovince. Excellent exposures in this area provide insights into development of the 3.0 Ga craton, an unconformable overlying 2.98 Ga rift sequence (Lewis-Storey assemblage) and the relationship of these North Caribou Terrane rocks to younger 2.73–2.72 Ga oceanic volcanic rocks (Black Island assemblage) and 2.72–2.71 Ga sedimentary rocks (Guano Island and Hole River).

Along the east shore of Lake Winnipeg, west-facing exposures of the 2.98 Ga Lewis-Storey rift-margin sequence lie unconformably on the ca. 3.0 Ga granitic basement, suggesting that an ocean basin opened at ca. 2.98 Ga on the west margin of the North Caribou Terrane. The west-facing Lewis-Storey and the east- and northeast-facing Black Island assemblages were subsequently juxtaposed during the 2.71–2.70 Ga collisional Uchian orogeny. The oblique nature of docking of these two terranes in the Black Island area may account for the generally excellent preservation state of primary features, as well as

formation of local depocentres attracting coarse clastic sediments (Guano Island and Hole River) in basins overlapping the collisional contact. Two subsequent deformational events, recorded in all supracrustal units, represent progressive strain increments accompanying final adjustments during the Uchian collision.

Similar to areas to the east at Bissett and Red Lake, the Black Island area has considerable potential for lode-gold mineralization. The context for this mineralization is much improved by the new mapping and improved structural understanding of the area. The rift-margin Lewis-Storey sequence has exploration potential for nickel and PGE. The diamond potential in the Black Island area and in the ancient North Caribou Terrane to the northeast has not been assessed. A possible arc-rifting event at the top of the Gray Point sequence on Lake Winnipeg and VMS-style alteration and sulphide fragments in volcanoclastic rocks near the top of the Bidou subgroup east of Bissett (Anderson, 2004) indicate that the Rice Lake greenstone belt may locally have potential to host base-metal mineralization.



## TABLE OF CONTENTS

	Page
Abstract .....	iii
Introduction .....	1
Regional setting and general geology .....	2
Description of units .....	4
North Caribou Terrane .....	4
East Shore Plutonic Complex .....	4
Tonalite (unit 1) .....	4
Diorite and quartz diorite (unit 2) .....	4
Lewis-Storey assemblage .....	4
Medium- to coarse-grained arkosic grit (unit 3) .....	5
Quartz arenite (unit 4) .....	5
Komatiite (unit 5) .....	5
Iron formation (unit 6) .....	5
Diabase and gabbro sills (unit 7) .....	8
Granodiorite (unit 8) .....	8
Continental-arc felsic magmatism .....	8
Biotite granodiorite to granite (unit 9) .....	9
Black Island assemblage .....	9
Gray Point sequence .....	10
Aphyric basalt and basaltic andesite (unit 10) .....	10
Porphyritic basalt and basaltic andesite (unit 11) .....	11
Intermediate to felsic volcanoclastic rocks (unit 12) .....	11
Drumming Point sequence .....	13
Basaltic andesite to andesite (unit 13) .....	13
Feldspathic wacke and related volcanoclastic rocks (unit 14) .....	14
Other rocks of the Black Island assemblage .....	16
Rhyolite tuff, lapilli tuff, breccia and rhyolite cobble conglomerate (unit 15) .....	16
Gabbro and quartz diorite (unit 16) .....	16
Sedimentary sequences of 2.71 Ga age .....	16
Guano Island sedimentary rocks .....	17
Boulder conglomerate (subunit 17a) .....	17
Arkose (subunits 17b and c) .....	18
Hole River sedimentary rocks .....	18
Arkose (unit 18) .....	18
Deformational events .....	20
D <sub>1</sub> deformation .....	20
D <sub>2</sub> deformation .....	20
D <sub>3</sub> deformation .....	21
Geochemistry of Black Island assemblage volcanic rocks .....	23
Mafic volcanic rocks .....	23
Felsic volcanic rocks .....	26
Economic geology .....	30

	<b>Page</b>
Discussion and Summary.....	30
Acknowledgments.....	31
References.....	31

## FIGURES

Figure 1: Major lithotectonic components of the western Superior Province in southeastern Manitoba and adjacent Ontario .....	1
Figure 2: Simplified geology of the study area, showing the distribution of the main rock sequences and structures .....	2
Figure 3: Dextral $D_1$ shear bands developed in tonalite (unit 1), East Shore Plutonic Complex, east shore of Lake Winnipeg....	4
Figure 4: Porphyroclastic gneiss enclave in weakly $D_1$ foliated hornblende-biotite quartz diorite (unit 1), East Shore Plutonic Complex, east shore of Lake Winnipeg.....	5
Figure 5: Schematic cross-section showing the stratigraphy of the Mesoarchean Lewis-Storey assemblage (units 3–7).....	6
Figure 6: Arkosic grit (unit 3) of the Lewis-Storey assemblage showing angular quartz and plagioclase detrital granules, island near east shore of Lake Winnipeg .....	6
Figure 7: Basal conglomeratic grit (unit 3) containing angular tonalite clasts in a chloritic matrix, Lewis-Storey assemblage, island near east shore of Lake Winnipeg .....	7
Figure 8: Fuchsitic quartzite (unit 4) of the Lewis-Storey assemblage, east shore of Lake Winnipeg .....	7
Figure 9: Quartzite pebbles in Lewis-Storey assemblage quartzite (unit 4).....	7
Figure 10: Komatiite flow (unit 5a) displaying spinifex texture defined by radiating clinopyroxene needles and fronds, Lewis-Storey assemblage, Lewis Island.....	8
Figure 11: Thinly laminated magnetite-chert iron formation (unit 6a), Lewis-Storey assemblage, Storey Island.....	8
Figure 12: Schematic stratigraphic section of the Black Island assemblage .....	9
Figure 13: Pillowed basalt (unit 10a) with increasing $D_1$ strain gradient toward left side of outcrop, Gray Point sequence, south shore of Black Island.....	10
Figure 14: Pillow-fragment breccia (unit 10a), Gray Point sequence .....	10
Figure 15: Quartz-carbonate vein stockworks in $D_1$ shear zone in basalt (unit 10c), Gray Point .....	11
Figure 16: Schematic stratigraphic section showing main features of a series of massive Gray Point mafic flows (unit 11a,e) ...	12
Figure 17: Zoned and partially resorbed plagioclase megacryst in massive basalt flow (unit 11b), Gray Point sequence, small island north of Black Island .....	12
Figure 18: Pegmatitic pod in massive gabbro-textured flow (unit 11c) prepared for sample collection for U-Pb dating, Gray Point sequence, small island north of Black Island .....	13
Figure 19: Normal size-grading at base of intermediate volcanoclastic bed (unit 12), Gray Point sequence, small island north of Black Island.....	13
Figure 20: Rounded rhyolite cobble in texturally immature intermediate greywacke matrix (unit 12), Gray Point sequence, small island north of Black Island .....	14
Figure 21: Rounded boulder of matrix-supported quartz-veined gabbro in 4 m thick debris flow bed (unit 12), Gray Point sequence, same location as Figure 20.....	14
Figure 22: Pillowed Drumming Point andesite (unit 13a), small island north of Black Island.....	15
Figure 23: Coarse greywacke (unit 14b) with angular lithic fragments, Drumming Point sequence, northeast shore of Black Island.....	15
Figure 24: Delicately laminated siltstone and mudstone (unit 14c) folded by $F_2$ , Drumming Point sequence, northeast shore of Black Island.....	15
Figure 25: Delicate apophyses on blocks in lapilli tuff-breccia (subunit 15a), south shore of Black Island.....	16
Figure 26: Reverse size-grading in rhyolite pebble conglomerate (subunit 15b), south shore of Black Island .....	17
Figure 27: Rhyolite fragment in subunit 15b, containing flattened pumice and shards, south shore of Black Island.....	17

Figure 28: Guano Island conglomerate (unit 17a) with rounded granitic cobble .....	18
Figure 29: Guano Island arkose (unit 17b) with isolated, $D_1$ -flattened, rounded granitic cobbles, on island near east shore of Lake Winnipeg .....	18
Figure 30: Trough crossbedded arkose (unit 18b), Hole River sedimentary rocks, on island due east of Adam Island .....	19
Figure 31: Trough crossbedded arkose (unit 18b) folded by $F_3$ , Hole River sedimentary rocks, same location as Figure 30 .....	19
Figure 32: Large-scale dextral shear bands in the layered sequence (unit 2), East Shore Plutonic Complex .....	20
Figure 33: Z-shaped $F_1$ folds transected by $S_1$ foliation, suggesting progressive fold development during incremental $D_1$ strain, $D_1$ shear zone in Gray Point basalt (unit 10b), Gray Point .....	21
Figure 34: Stretched-pebble conglomerate (flattened clasts indicated by arrows) of the Guano Island sequence, showing strong $S_1$ tectonic lamination, tight $F_1$ Z-folds and open $F_2$ crenulations, on an island between Black Island and east shore of Lake Winnipeg .....	21
Figure 35: Chlorite-carbonate-quartz schist developed in $D_1$ shear zone (unit 10b) on Gray Point.....	22
Figure 36: $F_3$ crenulation and folding of $D_1$ shear zone (unit 10b) on the small island directly northwest of Adams Island.....	22
Figure 37: Black Island assemblage volcanic rocks plotted on geochemical discrimination plots for rock type and major chemical affinities .....	23
Figure 38: Black Island assemblage basalt, basaltic andesite and andesite plotted on major- and trace-element discrimination diagrams .....	24
Figure 39: Black Island assemblage volcanic rocks plotted on various geochemical discrimination diagrams .....	25
Figure 40: Multi-element plots of Black Island assemblage and Bidou Lake subgroup mafic volcanic rocks normalized to normal mid-ocean ridge basalt (N-MORB) .....	26
Figure 41: Epsilon Nd ( $\epsilon_{Nd}$ ) value versus age for volcanic rocks of the Black Island assemblage and plutonic rocks of the East Shore Plutonic Complex .....	27
Figure 42: Gray Point basalt and basaltic andesite (units 10 and 11) plotted on a) Zr vs. Ti/100 vs. Y*3 (Pearce and Cann, 1973) and b) Th vs. Hf/3 vs. Ta (Wood, 1980) discriminant diagrams .....	27
Figure 43: Comparison of Black Island assemblage rhyolite with those of the 2.73 Ga Bidou Lake and 2.72 Ga Gem Lake volcanic assemblages, Rice Lake greenstone belt, on a granitic-rock discriminant plot of Y vs. Nb (Pearce et al., 1984) .....	28
Figure 44: Comparison of Black Island assemblage rhyolite with those of the 2.73 Ga Bidou Lake and 2.72 Ga Gem Lake volcanic assemblages, Rice Lake greenstone belt.....	28
Figure 45: Primitive-mantle-normalized (Sun and McDonough, 1989) extended-element plots of geochemical data for felsic rocks of the Rice Lake greenstone belt.....	29

## MAPS

GR2005-2-1: Geology of the Black Island–Seymourville area, Manitoba (parts of NTS 62P1, 7 and 8), 1:20 000 scale .....	back pocket
GR2005-2-2: Geology of the Pipestone Rock–Rice River area, Manitoba (parts of NTS 62P7 and 8), 1:20 000 scale .....	back pocket

## DIGITAL DATA

On CD-ROM inside back cover:

Geoscientific Report GR2005-2 and accompanying maps (GR2005-2-1 and -2) in PDF

Data Repository item DRI2005004: Lithogeochemical and lithological data, Sm-Nd isotopic data and geochronological data for the Black Island area, Lake Winnipeg, Manitoba (parts of NTS 62P1, 7 and 8) and the Rice Lake greenstone belt (parts of NTS 62P, 52M and 52L)<sup>1</sup>

<sup>1</sup> Also available online to download free of charge at [www2.gov.mb.ca/itm-cat/freedownloads.htm](http://www2.gov.mb.ca/itm-cat/freedownloads.htm) or on request from [minesinfo@gov.mb.ca](mailto:minesinfo@gov.mb.ca) or Mineral Resources Library, Manitoba Industry, Economic Development and Mines, 360–1395 Ellice Avenue, Winnipeg, MB R3G 3P2, Canada

## Introduction

The Black Island area on eastern Lake Winnipeg, which was previously mapped by Davies (1951), Ermanovics (1970, 1981) and Brown (1981), contains the most westerly exposures of the Uchi Subprovince (Figure 1). The area contains key tectonostratigraphic relationships between the Mesoarchean North Caribou Terrane, which includes an unconformable ca. 2.98 Ga rift sequence, a tectonically juxtaposed ca. 2.72 Ga oceanic volcanic package of the Uchi Subprovince and two ca. 2.71 Ga sedimentary overlap sequences that formed during but prior to culmination of the ca. 2.70 Ga Uchian orogeny.

Elucidation of the complex structural history along the boundary between the Mesoarchean rocks on the east shore of Lake Winnipeg and the Neoarchean volcanic rocks exposed on Black Island provides a much-improved geological context for understanding the evolution of the North Caribou and Uchi domains in Manitoba and adjacent Ontario. This domain interface and younger shear zones spatially associated with it are an

important locus for gold mineralization, including the important deposits at Bissett in Manitoba and Red Lake in Ontario. The previously unrecognized rift succession (Lewis-Storey assemblage) on the east shore of and beneath Lake Winnipeg, in combination with the large areal extent of older ca. 3.0 Ga crust, opens up new exploration possibilities for nickel, platinum group elements (PGE) and diamonds in this underexplored and previously poorly understood area.

Mapping of the Black Island area was conducted at 1:20 000 scale (GR2005-2-1 and GR2005-2-2, in pocket) during the summer of 2000 by J. Percival of the Geological Survey of Canada (GSC) and A. Bailes of the Manitoba Geological Survey (MGS; Bailes and Percival, 2000; Bailes et al., 2003). Follow-up work included geochronology by V. McNicoll (GSC), isotopic analysis by K. Tomlinson (GSC), tectonic synthesis by J. Percival (GSC) and geochemistry of the Black Island assemblage volcanic rocks by A. Bailes (MGS).

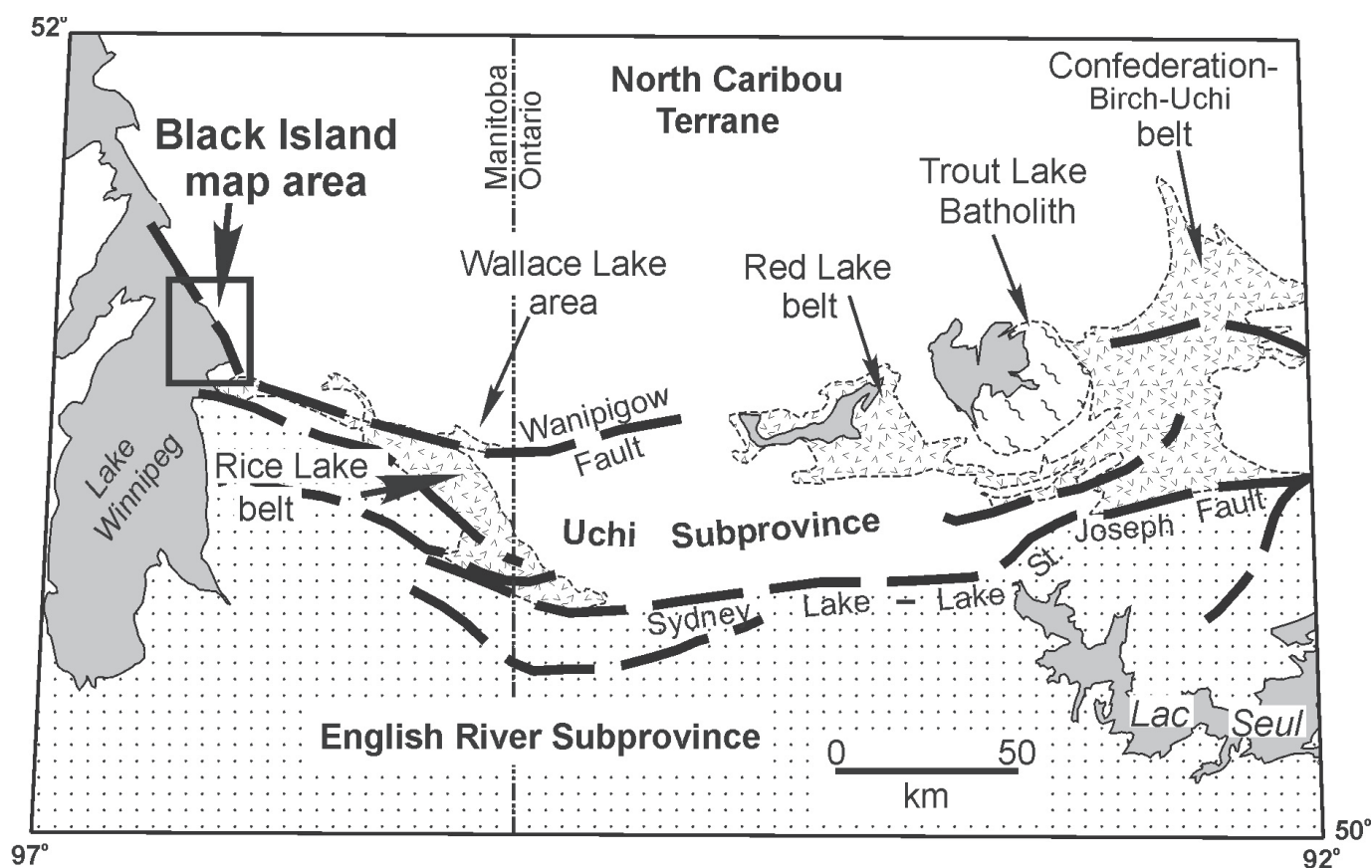


**Figure 1:** Major lithotectonic components of the western Superior Province in southeastern Manitoba and adjacent Ontario. The Black Island area, shown by the rectangle, is located on the east shore of Lake Winnipeg and straddles the interface between the Uchi Subprovince and the older North Caribou Terrane.

## Regional setting and general geology

Thurston et al. (1991) defined the North Caribou Terrane to consist of Mesoarchean tonalitic basement; an unconformable platform-rift succession of quartzite, carbonate, iron formation and komatiite; and 2.73–2.70 Ga granitoid plutonic rocks formed during a continental-arc magmatic episode. Extensive 2.73–2.70 Ga granitoid plutonism (Stone, 1998; Corfu and Stone, 1998) largely obscures the Mesoarchean basement and platform-rift successions such that they are only rarely documented along the southern flank of the North Caribou Terrane. One exception is on the east shore of Lake Winnipeg adjacent to Black Island, where these Mesoarchean sequences are exceptionally well exposed (Figure 2). They include the ca. 3.0 Ga

East Shore Plutonic Complex, the unconformably overlying ca. 2.98 Ga Lewis-Storey (rift-margin) assemblage and ca. 2.94 Ga granitoid rocks of unknown extent (Bailes and Percival, 2000; Percival et al., 2002).

The Uchi Subprovince, which consists of strands of Mesoarchean and Neoarchean volcanic rocks, includes the Red Lake, Birch-Uchi and Pickle Lake greenstone belts in Ontario and the Rice Lake greenstone belt in Manitoba. Tholeiitic and calc-alkaline Neoarchean volcanic rocks volumetrically dominate the Rice Lake belt and are represented in the Black Island area by the ca. 2.72 Ga Black Island assemblage. The latter is composed of the mainly homoclinal, east- to northeast-facing, Gray Point

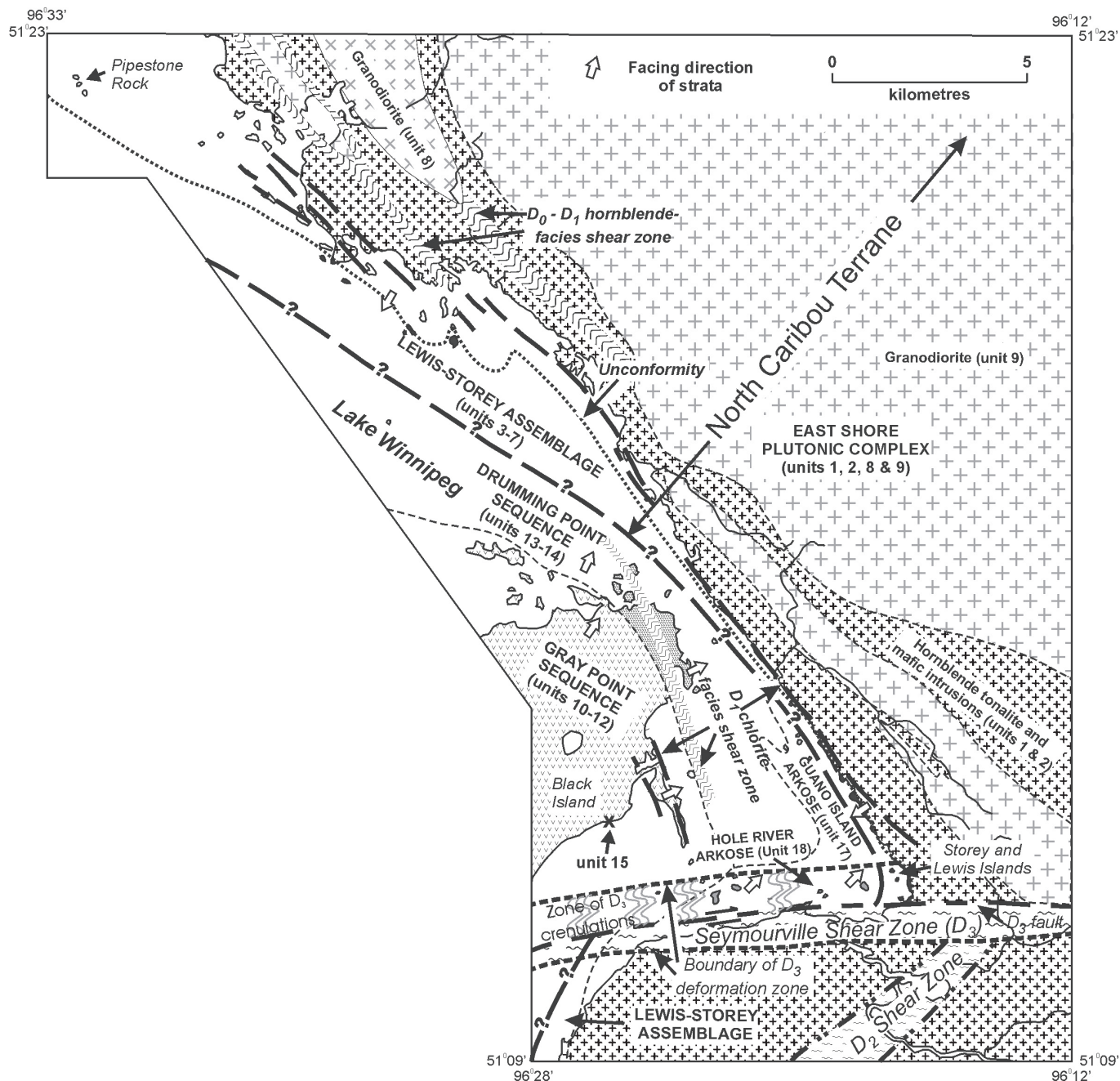


**Figure 2:** Simplified geology of the study area, showing the distribution of the main rock sequences and structures.



tholeiitic and Drumming Point calcalkalic sequences (Figure 2; see 'Geochemistry of Black Island assemblage volcanic rocks' section).

Rocks in the map area record three regional deformation events ( $D_1$ ,  $D_2$ ,  $D_3$ ), with local evidence of pre- $D_1$  deformation in the East Shore Plutonic Complex (Percival et al., 2001). The  $D_1$  event, which is interpreted to have accompanied juxtaposition of the East Shore Plutonic Complex and the Black Island assemblage, is represented by a regional, north-northwest-trending, steeply dipping schistosity and several discrete dextral transpressive shear zones paralleling the boundary. The  $D_2$  and  $D_3$  events are interpreted to represent, respectively, north-directed shortening and dextral translation on east-trending structures formed during the ca. 2.70 Ga Uchian orogeny.

The Uchian orogeny was accompanied by deposition of coarse clastic, arkosic overlap sequences along the boundary

of the North Caribou Terrane and the Uchi Subprovince, and coeval marine greywacke to the south in the English River Subprovince (Figures 1 and 2). In the Black Island area, the overlap sequences are represented by the <2722 Ma Guano Island and <2707 Ma Hole River sedimentary rocks. The Guano Island sedimentary rocks possess prominent  $D_1$ ,  $D_2$  and  $D_3$  structural fabrics, indicating that these deformational events are younger than 2722 Ma. The Hole River sedimentary rocks are interpreted to follow the main  $D_1$  event, as they have only weakly developed  $D_1$  fabrics. Well-developed  $D_2$  and  $D_3$  structures in the Hole River sedimentary rocks indicate that these structural events are younger than 2707 Ma.

The Phanerozoic rocks, which were not mapped during this project (contacts *from* Davies 1951; Brown, 1981) include a flat-lying cover of Winnipeg Formation sandstone and Red River Formation dolomite.

## Description of units

### *North Caribou Terrane*

A large domain of Mesoproterozoic rocks was identified east of Lake Winnipeg and north of the Wanipigow Fault (Figures 1 and 2) by Krogh et al. (1974), Turek et al. (1989), Turek and Weber (1994) and Poulsen et al. (1996). The generation of this 3006–2992 Ma continental crust is fully discussed by Whalen et al. (2003) and Ravenelle (2001). In the Black Island area, this older crustal domain is referred to as the East Shore Plutonic Complex (Bailes and Percival, 2000; Percival et al., 2002).

### **East Shore Plutonic Complex**

Two main units characterize the East Shore Plutonic Complex. A 1–2 km wide linear body of homogeneous hornblende-biotite tonalite (unit 1) underlies the east shore of Lake Winnipeg and its eastern islands. It grades to the east into a layered complex of tonalite, quartz diorite and diorite (unit 2), with sheets of gabbro, pyroxenite and hornblendite. All units carry a moderate to strong northwest-striking foliation, with intense deformation in  $D_1$  shear zones. A pre- $D_1$  foliation is evident in a few outcrops.

### ***Tonalite (unit 1)***

The hornblende tonalite (unit 1) is coarse to medium grained, with characteristic blue quartz and plagioclase phenocrysts up to 1 cm on the long axis. Where primary features are preserved, the rock is equigranular to plagioclase porphyritic, with 10–15% biotite and 5–10% hornblende.

Extensional shear bands are well developed, along with sporadic C-S fabrics, in  $D_1$  greenschist-facies shear zones (Figure 3). These zones are characterized by the alteration of hornblende and biotite to chlorite. In a few outcrops, the low-grade shear zones overprint an older, ductile, east-trending foliation.

Rare enclaves (Figure 4) within the tonalite may represent an ancient supracrustal sequence (Ermanovics, 1970). Two

exposures in the Rice River bay area contain such older relicts. In one, the tonalite contains lenticular enclaves (on the order of 2.0 by 0.2 m) of fine-grained schistose sandstone with a strong east-west foliation that is transected by  $D_1$  chloritic shear zones. Foliated ( $S_1$ ) quartz diorite in the second exposure hosts a 1 by 2 m enclave of migmatitic porphyroclastic gneiss. Pre- $D_1$  folds of the mylonitic layering are truncated at the enclave margin. These rare examples provide evidence for a significant geological history predating emplacement of the East Shore Plutonic Complex.

### ***Diorite and quartz diorite (unit 2)***

The layered complex (unit 2) is composed mainly of hornblende-biotite quartz diorite, with sheets of more mafic composition that are on the order of 1–20 m. Blue quartz (<10%) characterizes the homogeneous, medium-grained quartz diorite, which contains 10–20% biotite and 15–25% hornblende.

High-strain ( $D_1$ ) zones in the layered complex generally form in quartz diorite and diorite units, where deformation features range from broad (approx. 100 m) zones of flaser to augen foliation at lower strain levels, to narrow (1–10 m) protomylonite and mylonite zones at higher strains. Gabbro, pyroxenite and hornblendite generally preserve coarse igneous textures.

### **Lewis-Storey assemblage**

The Lewis-Storey assemblage (Figures 2 and 5) is a steeply dipping, westward-younging sedimentary-volcanic (komatiite) sequence exposed along the eastern shore of Lake Winnipeg. These rocks are similar to a <3.0 to >2.92 Ga succession of quartzite, iron formation and komatiite at Wallace Lake (Poulsen et al., 1996; Sasseville and Tomlinson, 2000). At six low-strain localities over 30 km of strike length, an unconformity separates basement tonalite (unit 1) from this overlying sedimentary-volcanic sequence (units 3–6).

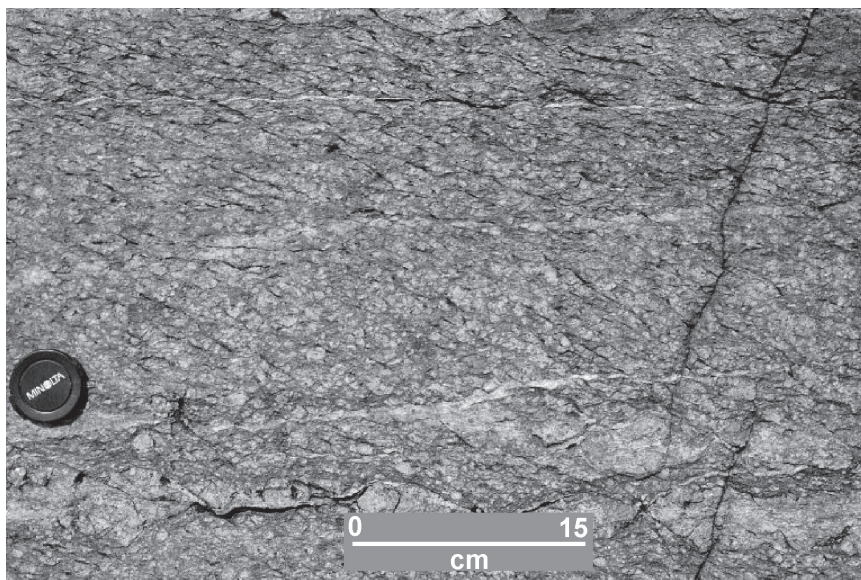


**Figure 3:** Dextral  $D_1$  shear bands developed in tonalite (unit 1), East Shore Plutonic Complex, east shore of Lake Winnipeg.





**Figure 4:** Porphyroclastic gneiss enclave in weakly D<sub>1</sub> foliated hornblende-biotite quartz diorite (unit 1), East Shore Plutonic Complex, east shore of Lake Winnipeg.

The Lewis-Storey assemblage is interpreted to mark the ancient (ca. 2.98 Ga; Percival et al., 2002, work in progress 2005) rifted margin of the North Caribou Terrane. Basal grit (unit 3) may have developed through chemical weathering and slight downslope transport of weathered tonalite basement during uplift preceding rifting (cf. Rainbird and Ernst, 2001). Deposition of quartzite (unit 4) and carbonate-bearing iron formation (unit 6) may reflect shallow basins established as a result of thermal subsidence. The presence of komatiite (unit 5), together with stratigraphic evidence of early uplift and weathering, support a model of plume-driven rifting.

#### ***Medium- to coarse-grained arkosic grit (unit 3)***

The arkosic grit (unit 3) forms a 15–40 m thick unit of massive to thickly bedded grit composed of angular quartz and plagioclase detritus with up to 10% chloritic matrix (Figure 6). Near the base of this generally unsorted grit are local angular pebbles and cobbles of the basement hornblende-bearing tonalite (Figure 7).

At one locality, a 1.5 m thick quartz porphyritic sill cuts

the arkosic grit within a few metres of the basal unconformity. Prismatic to equant zircons from this sill yielded an upper intercept age of  $2978 \pm 3$  Ma (Percival et al., 2002, work in progress 2005), interpreted to be the crystallization age. This date provides a minimum age for the lower part of the Lewis-Storey assemblage.

#### ***Quartz arenite (unit 4)***

The quartz arenite (unit 4) includes thinly laminated, fine-grained quartzite with fuchsitic horizons (Figure 8). This unit is up to several metres thick and has an abruptly transitional lower contact with the underlying grit (unit 3) and is locally associated with muscovitic, aluminous and talc-bearing schists. Its upper contact with overlying units is not exposed. Well-rounded pebbles of fine-grained cherty quartzite (Figure 9) attest to the detrital origin of this unit.

Ages of detrital zircons from a sample of clean quartzite, determined by sensitive high-resolution ion microprobe (SHRIMP), provide a minimum age estimate of 2980 Ma for unit 4 (Percival et al., work in progress 2005). Many of the detrital zircon ages resemble those of the underlying basement (units 1 and 2), but include others that are slightly younger. The latter ages may indicate some lead loss from basement-derived zircons, or could represent a suite of rift-related volcanic units (Percival et al., 2002). The age-spread of the detrital zircons is most consistent with derivation from rocks of the directly underlying basement.

#### ***Komatiite (unit 5)***

Komatiite flows with clinopyroxene spinifex (unit 5a; Figure 10) and characterized by 20% MgO and a flat trace-element pattern (DRI2005004, Table 1) are exposed on Lewis Island. Ultramafic rocks lacking spinifex texture (unit 5b), presumed to be derived from komatiitic flows, are exposed along the east shore of Lake Winnipeg to the north of Lewis Island.

#### ***Iron formation (unit 6)***

Iron formation with associated carbonate and siliceous sedimentary rocks (unit 6) overlie and are locally intercalated with the komatiite flows (unit 5). Thinly laminated magnetite-chert iron formation (Figure 11; unit 6a), exposed on Storey Island, consists of millimetre- to centimetre-scale layers of carbonate, chert, magnetite and sericite schist. Carbonate and siliceous sedimentary rocks with muscovite laminae (unit 6b) are exposed on both Lewis and Storey islands. Although unit 6 sedimentary rocks are only exposed on these two islands, aeromagnetic data and local diamond-drill intersections (Assessment Files 93757, 94532, Manitoba Industry, Economic Development and Mines, Winnipeg) show that the iron formation, related sedimentary rocks and associated komatiite flows likely extend for at least 30 km to the north-northwest of Lewis and Storey islands.



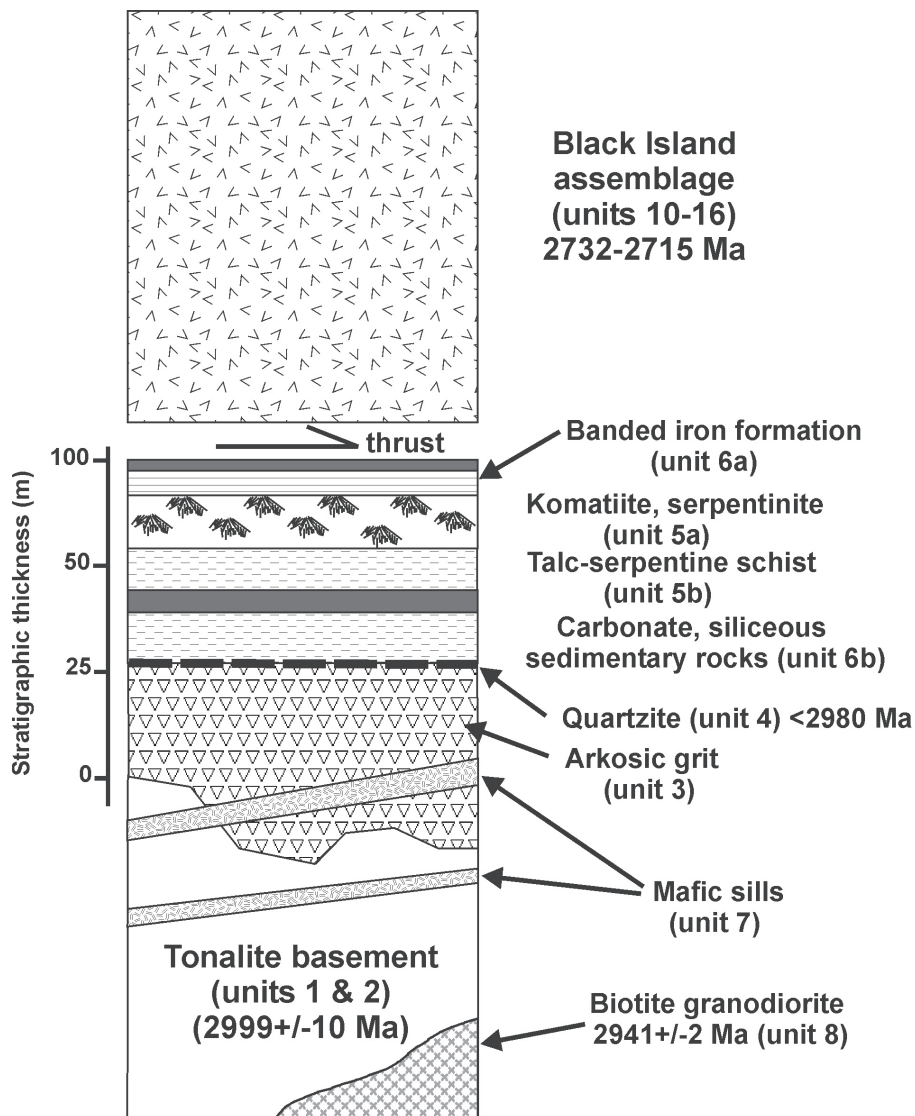


**Figure 5:** Schematic cross-section showing the stratigraphy of the Mesoproterozoic Lewis-Storey assemblage (units 3–7). The east-facing Lewis-Storey assemblage, a probable platform-rift sequence, lies unconformably on ca. 3.0 Ga tonalitic basement (units 1–2) and is in structural contact with Neoproterozoic volcanic rocks of the Black Island assemblage (units 9–15). Unit numbers correspond to those on the geological maps (GR2005-2-1 and GR2005-2-2, in pocket).



**Figure 6:** Arkosic grit (unit 3) of the Lewis-Storey assemblage, showing angular quartz and plagioclase detrital granules, island near east shore of Lake Winnipeg. The grit displays a prominent  $D_1$  foliation and dextral shear bands.



**Figure 7:** Basal conglomeratic grit (unit 3), containing angular tonalite clasts in a chloritic matrix, Lewis-Storey assemblage, island near east shore of Lake Winnipeg. Hornblende is preserved in the tonalite clasts, whereas the detrital matrix between clasts contains only chlorite. A prominent  $D_1$  foliation and dextral shear bands are preferentially developed in the detrital matrix.

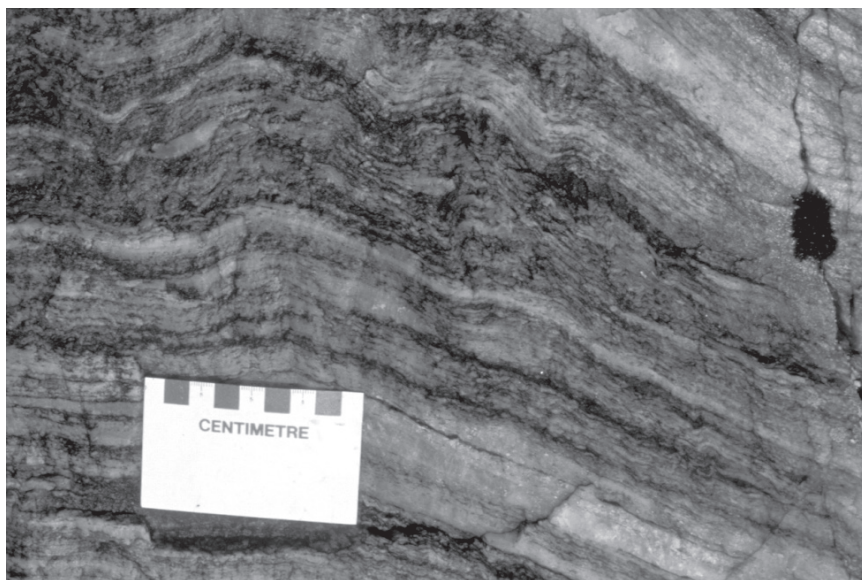
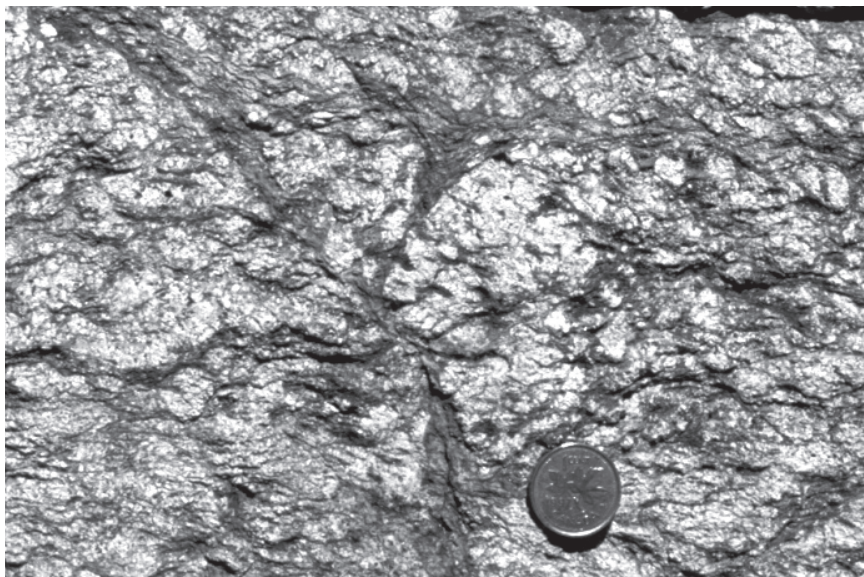


**Figure 8:** Fuchsitic quartzite (unit 4) of the Lewis-Storey assemblage, east shore of Lake Winnipeg. Bedding ( $S_0$ ), which strikes northwest, is accentuated by bedding-parallel  $S_1$ . The open folds, which trend southwest, are  $F_2$ .

**Figure 9:** Quartzite pebbles in Lewis-Storey assemblage quartzite (unit 4), east shore of Lake Winnipeg.

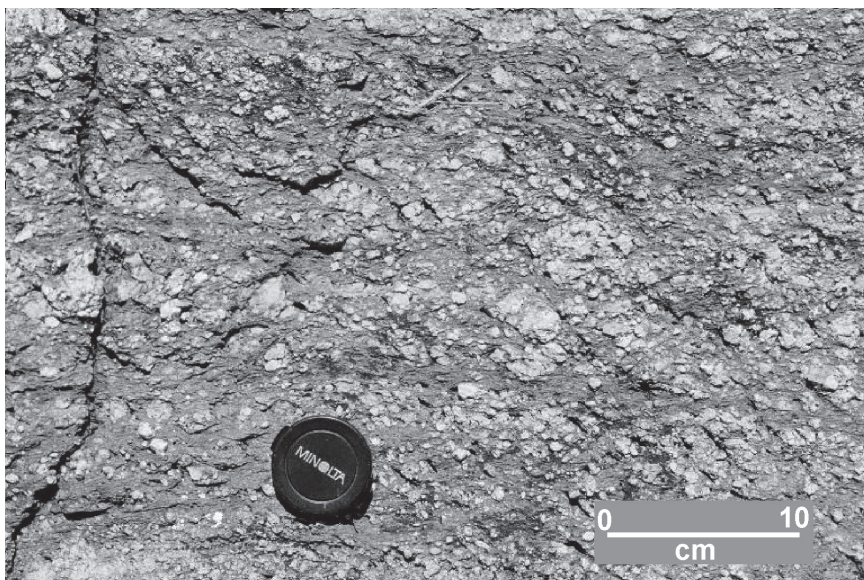




**Figure 10:** Komatiite flow (unit 5a) displaying spinifex texture defined by radiating clinopyroxene needles and fronds, Lewis-Storey assemblage, Lewis Island.

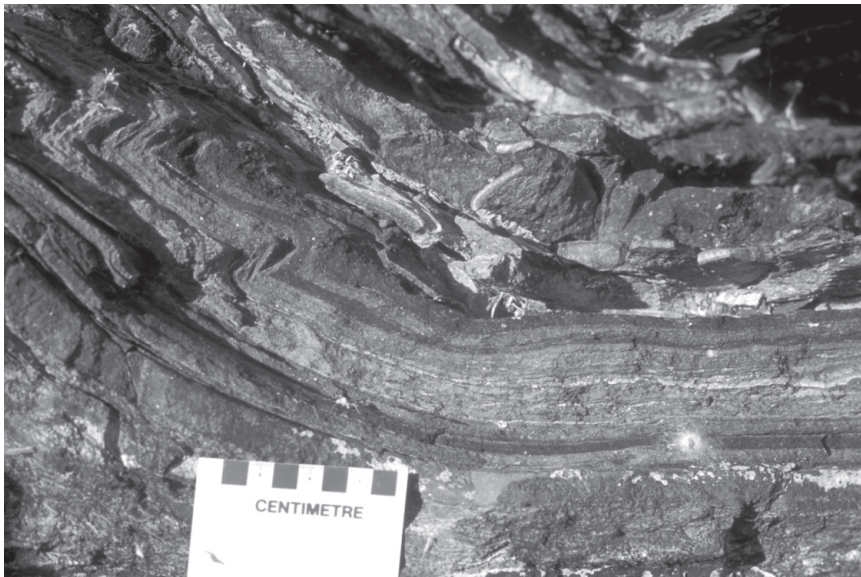
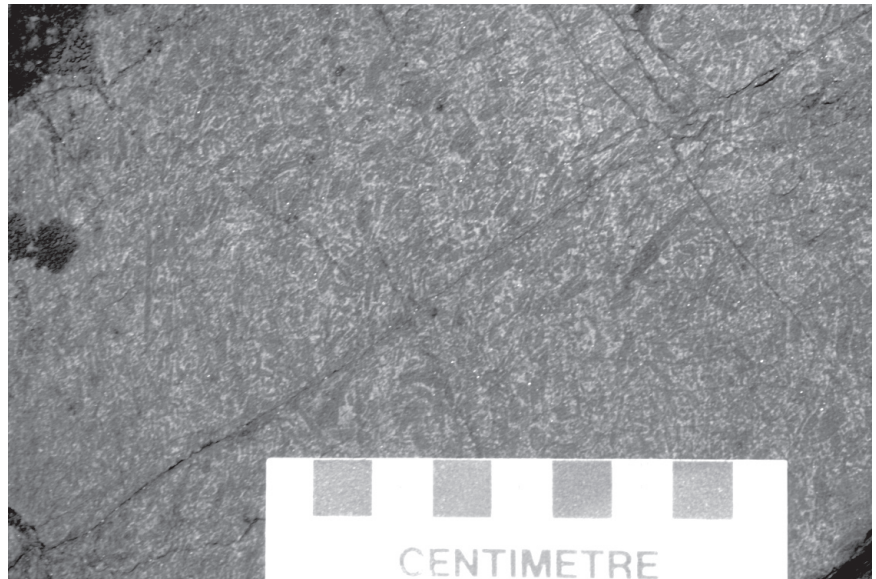


**Figure 11:** Thinly laminated magnetite-chert iron formation (unit 6a), Lewis-Storey assemblage, Storey Island.

#### ***Diabase and gabbro sills (unit 7)***

Unit 7 mafic sills and dikes up to 15 m thick intrude both the East Shore Plutonic Complex and the Lewis-Storey assemblage within a few hundred metres of their unconformable contact. The sills and dikes have N-MORB geochemistry (DRI2005004, Table 1), are generally fine to medium grained, and have chilled margins up to 50 cm wide. The mafic sills and dikes are interpreted as possible expressions of rift-related magmatism. Local felsic sills, one yielding an upper intercept age of  $2978 \pm 3$  Ma (Percival et al., 2002, work in progress 2005) and giving a minimum age for the Lewis-Storey assemblage, are also present but too small to be mapped.

#### ***Granodiorite (unit 8)***

Some early northwest-striking shear zones in units 1 and 2 of the East Shore Plutonic Complex are transected by dikes and larger bodies of medium-grained biotite granodiorite. One of these weakly foliated, medium-grained biotite granodiorite

bodies provided a concordant zircon age of  $2941 \pm 2$  Ma, taken as the crystallization age (Percival et al., work in progress 2005). This body has been distinguished on the map as unit 8. During mapping, this biotite granodiorite was not distinguishable from younger continental-arc biotite granodiorite (unit 9). For this reason, unit 8 granodiorite has not been identified on the map with the exception of the dated intrusion. The ca. 2941 Ma granodiorite (unit 8) is important, as it records a Mesoarchean episode of felsic plutonism in the East Shore Plutonic Complex that postdates both the Lewis-Storey assemblage and an early episode of deformation ( $D_0$ ).

#### ***Continental-arc felsic magmatism***

The North Caribou Terrane is intruded by 2.73–2.70 Ga hornblende- and biotite-bearing quartz diorite, tonalite, granodiorite and local quartz monzonite (Marr, 1971, Ermanovics, 1981; Stone, 1998). These plutons have been interpreted to represent continental-arc magmatism at an Andes-type

continental margin (Poulsen et al., 1996; Stone, 1998; Percival and Whalen, 2000).

### ***Biotite granodiorite to granite (unit 9)***

Medium- to coarse-grained biotite granodiorite (unit 9) intrudes the East Shore Plutonic Complex east of Lake Winnipeg. Although this unit was locally examined and intrusive age relationships to other units of the East Shore Plutonic Complex established, its distribution is largely from the previous mapping by Davies (1951), Ermanovics (1970, 1981) and Brown (1981). Unit 9 likely contains bodies of the older biotite granodiorite (unit 8) but, with the exception of the intrusion that

gave an age of 2.941 Ga, these bodies have not been dated and cannot be distinguished on the map. A dike of the K-feldspar augen phase of unit 9 from the east shore of Lake Winnipeg contains zircons with an imprecise upper intercept age of  $2715 \pm 10$  Ma, interpreted as the crystallization age (Krogh et al., 1974).

### ***Black Island assemblage***

The Black Island assemblage consists of lower greenschist facies volcanic and volcanoclastic rocks that form a steeply dipping, homoclinal, northeast-facing succession more than 3 km thick (Figure 12). The degree of deformation of Black

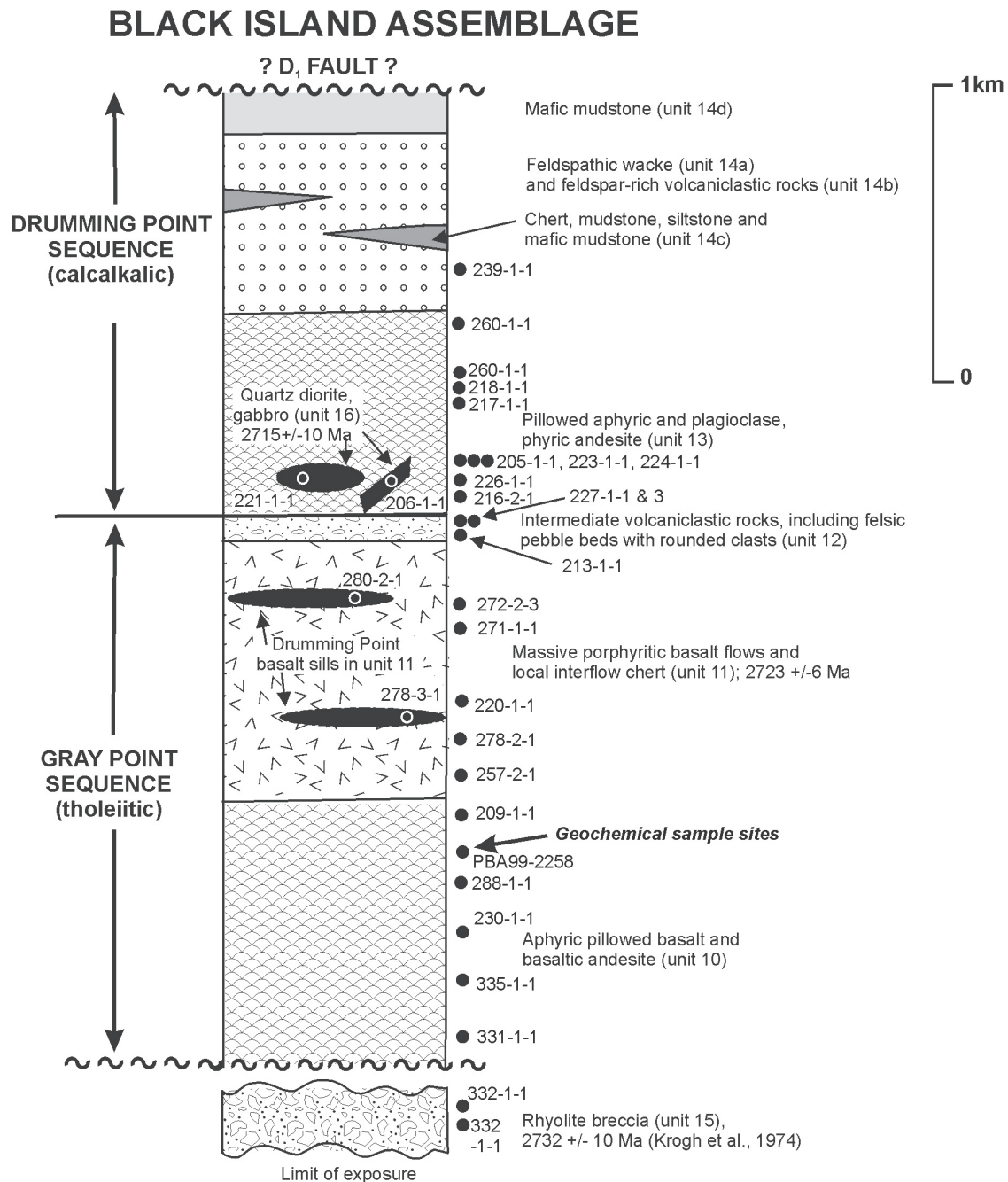


**Figure 12:** Schematic stratigraphic section of the Black Island assemblage. Unit numbers correspond to those on maps GR2005-2-1 and GR2005-2-2 (in pocket). Black dots with numbers to the right of the stratigraphic column are geochemical samples.



Island assemblage rocks increases toward the east and toward the contact with the adjacent North Caribou Terrane. More strongly deformed units on eastern Black Island and on islands to the east are characterized by a north- to north-northwest-trending  $S_1$  foliation and local discrete  $D_1$  shear zones.

The lower third of the section, termed the Gray Point sequence, consists of tholeiitic basalt and basaltic andesite flows (units 9 and 10) with an 80–120 m thick cap of volcanoclastic rocks and minor rhyolite (unit 11). The upper two-thirds, termed the Drumming Point sequence, comprise calcalkaline andesitic flows (unit 12) and associated volcanoclastic rocks (unit 13).

A 260 m.y. ‘time gap’ separates the northeast-facing, ca 2.72 Ga Black Island assemblage (units 9 to 15) to the west from the ca 3.0 Ga Mesoarchean basement (units 1 and 2) and its southwest-facing >2.98 Ga cover strata (units 3 to 7) of the North Caribou Terrane to the east. The juxtaposition of the juvenile, tholeiitic and calcalkaline submarine volcanic rocks of the Black Island assemblage to the North Caribou margin is

interpreted to have occurred along a transpressive  $D_1$  deformation zone whose margins are observed in outcrop and drillcore (GR2005-2-1 and GR2005-2-2, in pocket).

### Gray Point sequence

#### *Aphyric basalt and basaltic andesite (unit 10)*

This unit, more than 1000 m thick, consists of aphyric basalt and basaltic andesite flows (subunit 10a) and mafic tectonite derived through  $D_1$  strain (subunit 10b). The least deformed basalt and basaltic andesite of subunit 10a are exposed in small outcrops along the north and south shorelines of Black Island. These flows are characterized by medium to dark grey-green colour on both fresh and weathered surfaces, an absence of vesicles, and ubiquitous pillow structures (Figure 13) with thin (<1 cm) selvages (dark green) and inter-pillow hyaloclastite domains. Monolithic pillow-fragment breccia (Figure 14) was observed in small outcrops on the north shore of Black Island. One pillowed flow displayed



**Figure 13:** Pillowed basalt (unit 10a) with increasing  $D_1$  strain gradient toward left side of outcrop, Gray Point sequence, south shore of Black Island.

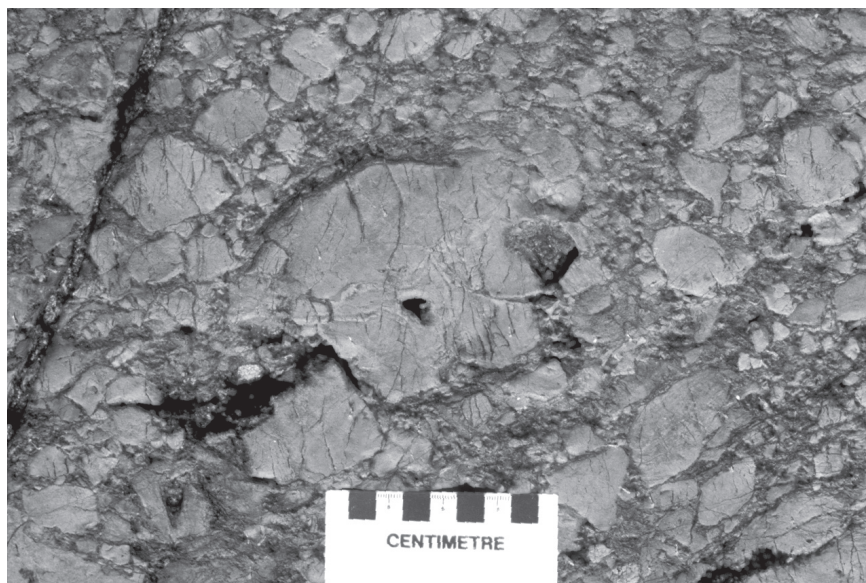


**Figure 14:** Pillow-fragment breccia (unit 10a), Gray Point sequence, north shore of Black Island. Note curving broken pillow margin in clast above scale card. The oxidized broken pillow selvage at the margin of this fragment is typical of pillow-fragment breccia.



well-developed thermal contraction cracks and radial pipe vesicles. Because of the small size of subunit 10a outcrops, no information is available on flow thicknesses or internal flow organization. No interflow sedimentary or tuff units were observed.

Laminated mafic tectonite (unit 10b) forms north-trending and steeply dipping  $D_1$  shear zones in the Gray Point sequence. Foliated pillowed basalt (subunit 10a) grades over a few metres into mafic tectonite (subunit 10b; Figure 13). On Gray Point, the  $D_1$  mafic tectonite and shear zones contain numerous quartz-carbonate-chlorite vein stockworks (Figure 15) that may have potential for gold mineralization. Samples from two sites indicated Au values to be less than 8 ppb, but further sampling is warranted.

### ***Porphyritic basalt and basaltic andesite (unit 11)***

This 700–1200 m thick unit consists of massive basalt and basaltic andesite flows (unit 11) that weather pale buff-brown to rarely dark grey-green and are pale grey-green to rarely dark green on fresh surfaces. Least deformed exposures of this unit occur on islands directly north of Black Island; more

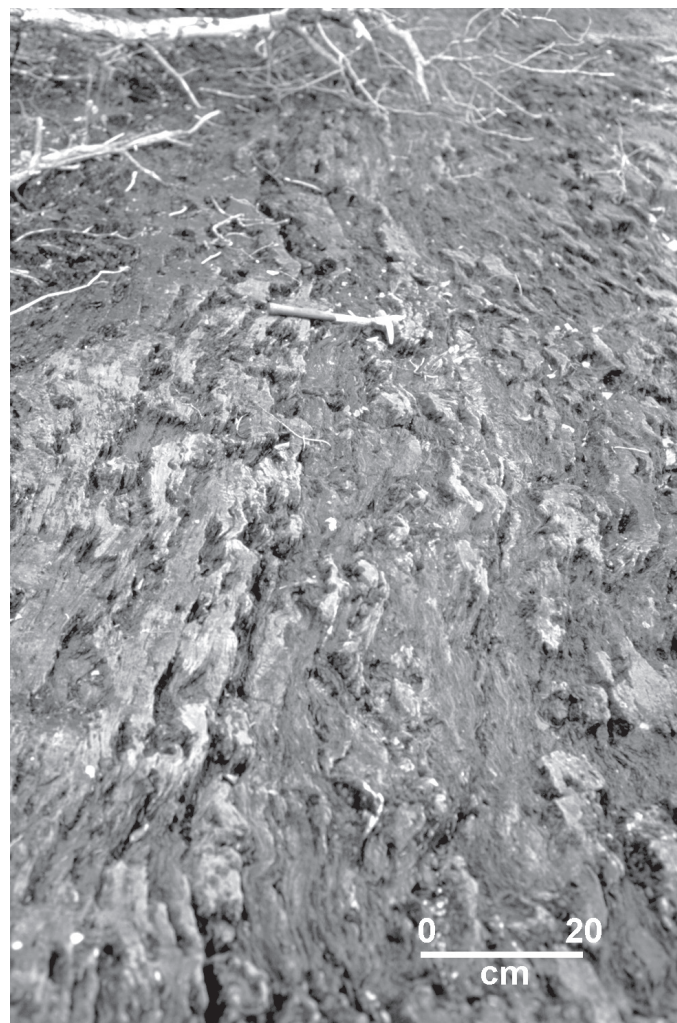


**Figure 15:** Quartz-carbonate vein stockworks in  $D_1$  shear zone in basalt (unit 10c), Gray Point. Note east-trending open  $F_3$  flexures of the  $S_1$  fabric.

deformed and less well exposed outcrops occur on small islands east of Gray Point. The flows contrast with those of unit 10, as they are porphyritic and massive, and commonly display up to 3 m thick interflow chert units (Figure 16). The interflow chert units increase in both abundance and thickness stratigraphically up through this 700–1200 m thick succession. The flows lack amygdules and pillow structures, and contain only rare spherulites. Flow contacts are defined by chilled margins; thick massive flows commonly display subtle variations in grain size that may be a consequence of incomplete cooling and amalgamation of flow units. Measured flows vary in thickness from 13 to >60 m.

Most of the flows are pyroxene and pyroxene+plagioclase phyrlic (unit 11a), with up to 40% 2–8 mm phenocrysts or oikocrysts. Less common are plagioclase megacrystic (unit 11b; 1–5 cm, rarely to 12 cm) and pyroxene glomerocrystic (unit 11c; <4 cm) flows. Plagioclase megacrysts locally display zoning and resorbed margins (Figure 17). Pyroxene glomerocrysts in subunit 11d are up to 4 cm in diameter.

Thick flows are locally gabbro textured and rarely pegmatitic. A pegmatite pod (Figure 18) from one thick flow was collected for U-Pb zircon dating and yielded very small quantities of zircon; two multigrain fractions of anhedral fragments were analyzed. One point is concordant at  $2723 \pm 6$  Ma (Percival et al., work in progress 2005), interpreted as the age of the Gray Point sequence.

### ***Intermediate to felsic volcanoclastic rocks (unit 12)***

This 80–120 m thick unit is composed dominantly of bedded, intermediate volcanoclastic rocks rich in plagioclase phenocrasts (unit 12a). In addition, it contains chert, siliceous sedimentary rocks and heterolithic intermediate to felsic volcanic conglomerate (unit 12b), as well as rare rhyolite breccia and pillowed plagioclase-phyric basaltic andesite flows. Chert beds (unit 12c), which occur sporadically throughout unit 12, suggest periodic sediment starvation of the depositional basin. The presence of soft-sediment slumping of chert in one locality suggests basin instability during lithification.

Unit 12 is interpreted to belong to the Gray Point sequence because it is cut by local dikes and sills of pyroxene and plagioclase-phyric gabbro that are texturally identical to Gray Point basalt flows. The intrusions locally display amoeboid margins consistent with synvolcanic intrusion into unconsolidated sedimentary detritus. They contain oikocrysts of pyroxene, more consistent with an affiliation with Gray Point mafic magmatism than with the overlying Drumming Point mafic flows (unit 13), which lack pyroxene phenocrysts. Unit 12 is interpreted to correspond to a pause in the mafic magmatism with local construction of, or uplift of, volcanic rocks into a subaerial regime, combined with erosion and redeposition of detritus in a marine environment.

The intermediate volcanoclastic rocks (unit 12a) are composed of 10–100 cm thick beds displaying normal size-grading (Figure 19), basal scours, Bouma AB bed zoning and rare flame structures and rip-ups. They are typically composed of texturally immature sand and grit, and most likely represent

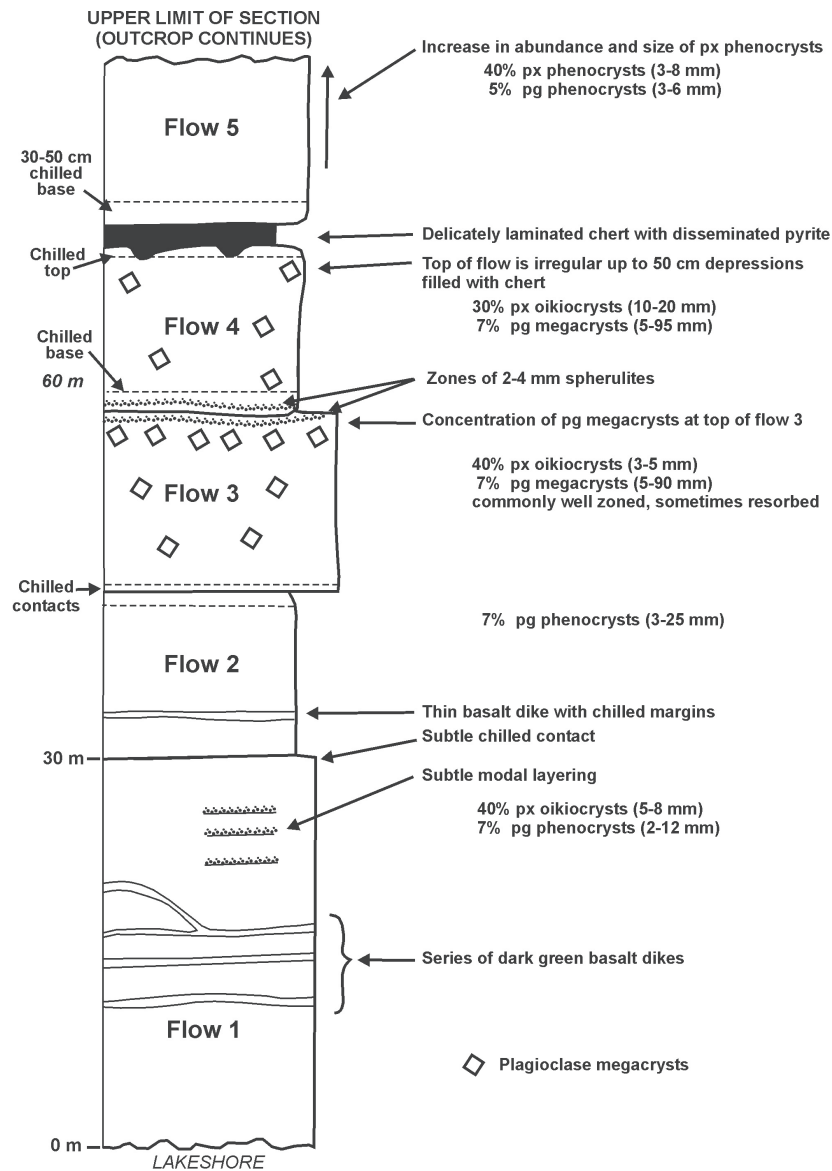


**Figure 16:** Schematic stratigraphic section showing main features of a series of massive Gray Point mafic flows (unit 11a,e). Abbreviations: pg, plagioclase; px, pyroxene.

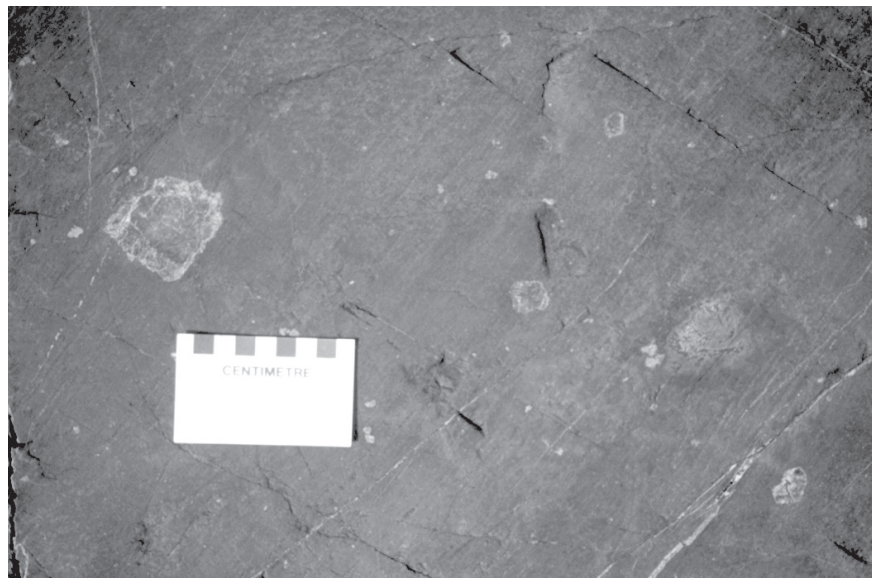


**Figure 17:** Zoned and partially resorbed plagioclase megacryst in massive basalt flow (unit 11b), Gray Point sequence, small island north of Black Island.



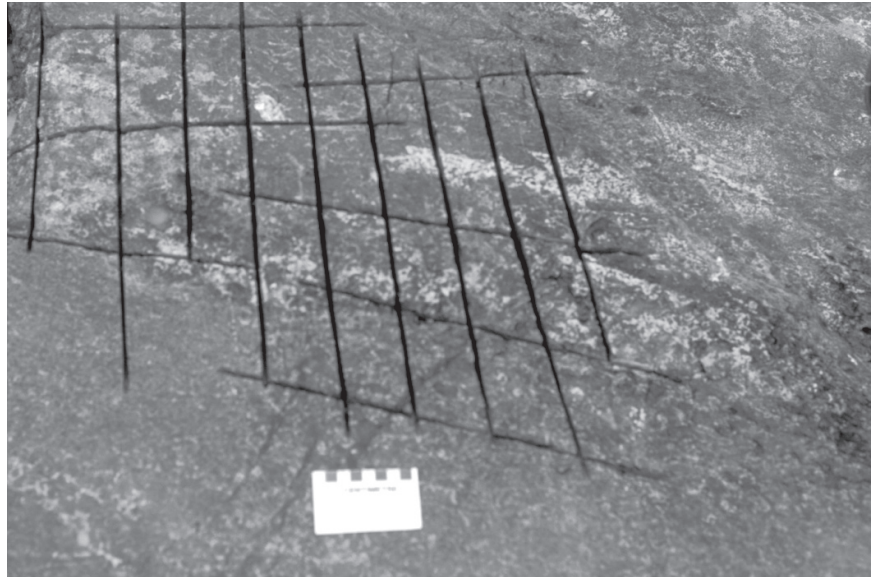


**Figure 18:** Pegmatitic pod in massive gabbro-textured flow (unit 11c), prepared for sample collection for U-Pb dating, Gray Point sequence, small island north of Black Island.

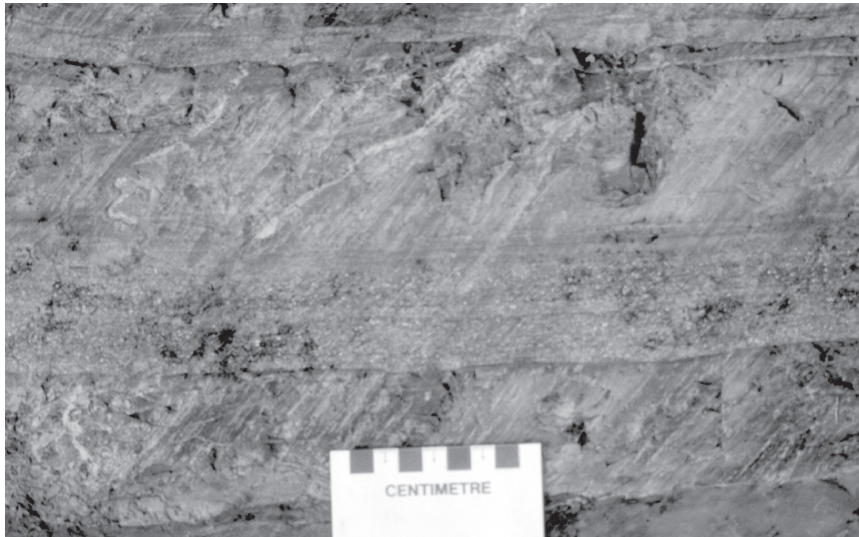


**Figure 19:** Normal size-grading at base of intermediate volcanoclastic bed (unit 12), Gray Point sequence, small island north of Black Island.

locally derived, unconsolidated volcanic detritus that slumped and was deposited subaqueously by turbidity currents.

Intercalated with the intermediate volcanoclastic turbidite units are volcanic conglomerate and breccia (subunit 12b) that form beds ranging from 1 m to more than 4 m in thickness; vary widely in composition and texture; contain a heterolithic clast population, including intrusive rocks; are matrix supported; and locally display both reverse and normal size-grading. Pebbles and cobbles in these beds are generally rounded to well rounded (Figure 20), in contrast to the clastic matrix, which is generally texturally immature. Rounding of pebbles and cobbles, heterolithic clast populations and presence of rare intrusive clasts (Figure 21) suggest unroofing of the source terrane, possible subaerial transport of clasts, and mixing prior to their incorporation in the volcanic conglomerate beds. The texturally immature character of the clastic matrix indicates that it likely had a local derivation and only limited, if any, subaerial transport.

## Drumming Point sequence

### *Basaltic andesite to andesite (unit 13)*

This 350–1100 m thick unit, which represents a resurgence of mafic volcanism, is composed of aphyric (subunit 13a) and less common plagioclase-phyric (subunit 13b; <10% phenocrysts, 0.5–3 mm in size) basaltic andesite and andesite flows. The flows are buff to buff-brown on weathered surfaces and medium to pale grey-green on fresh surfaces. They are least deformed (subunit 13a) on islands directly north of Black Island.

Most of the flows are pillowed (subunits 13a, b; Figure 22) and only rarely massive (subunit 13c). Flow thicknesses are not well constrained due to incomplete exposure of flows on small islands. Pillow selvages are typically less than 1 cm and interpillow hyaloclastite is typically between 1 and 4 cm thick. The flows contain rare amygdules, radial pipe vesicles and synvolcanic dikes. Interflow sedimentary deposits, which



**Figure 20:** Rounded rhyolite cobble in texturally immature intermediate greywacke matrix (unit 12), Gray Point sequence, small island north of Black Island.

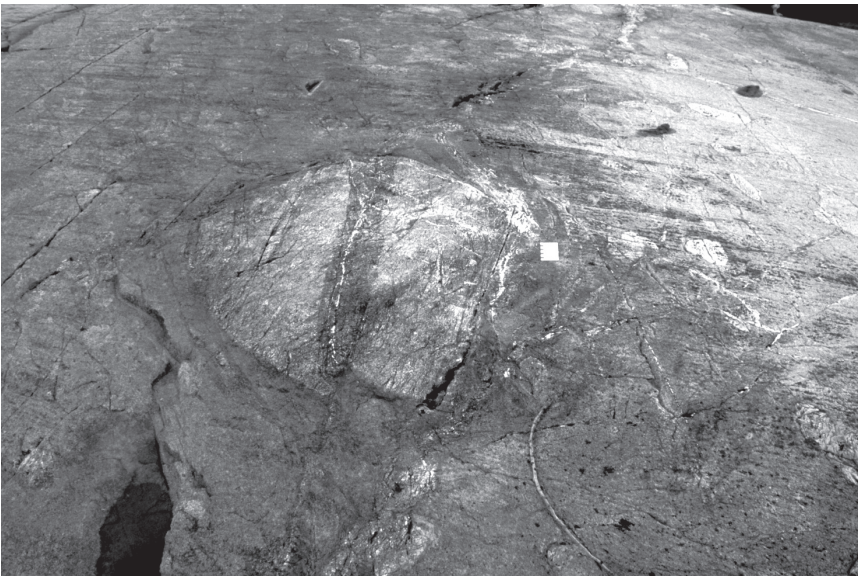
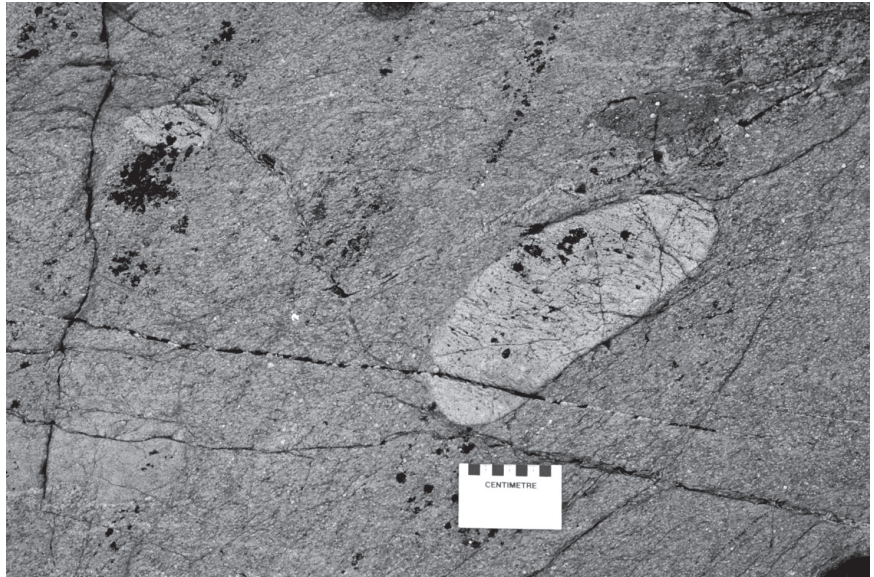


**Figure 21:** Rounded boulder of matrix-supported quartz-veined gabbro in 4 m thick debris flow bed (unit 12), Gray Point sequence, same location as Figure 20.

are common between Gray Point massive flows (unit 11), are absent in unit 13 flows.

Pillowed flows on islands east of Gray Point are commonly strongly foliated, and many of the flows have been tectonized (subunit 13d), with lensoid domains in which strongly flattened pillow relicts are preserved.

#### ***Feldspathic wacke and related volcanoclastic rocks (unit 14)***

The Drumming Point sequence is topped by up to 1000 m of feldspathic wacke and associated volcanoclastic rocks (unit 14). The thickness of this unit is not well constrained, as its eastern contact is unexposed and may be a D<sub>1</sub> fault. A sample of this unit, collected for detrital zircon dating, contained no zircon, suggesting that these sedimentary rocks were derived from a zircon-poor source terrane, likely the Black Island assemblage. The lack of zircons suggests deposition in a location

remote from the East Shore Plutonic Complex, which is presently situated only a few hundred metres to the east.

The sequence is dominated by feldspathic wacke (subunit 14a) and a massive, medium-grained, feldspathic volcanoclastic equivalent (subunit 14b). Both subunits 14a and b are characterized by buff to pale buff weathering and a medium grey-green fresh surface. Deformed equivalents are typically pale grey-green on both weathered and fresh surfaces. Orange-pink feldspars, likely saussuritized and hematized, generally form between 50 and 75% by volume of both these subunits, with the remainder consisting of amphibole and 5–20% quartz. The feldspathic wacke (subunit 14a) is typically well laminated but, because of its very limited variation in grain size, rarely forms well-defined beds. It locally displays normal size-grading, scours and flame structures, and contains rare fine-grained lithic pebbles (Figure 23). Locally, it is intercalated with fine-grained siltstone, chert and mafic mudstone (subunit 14c; Figure 24). Crystal-rich feldspathic volcanoclastic rocks



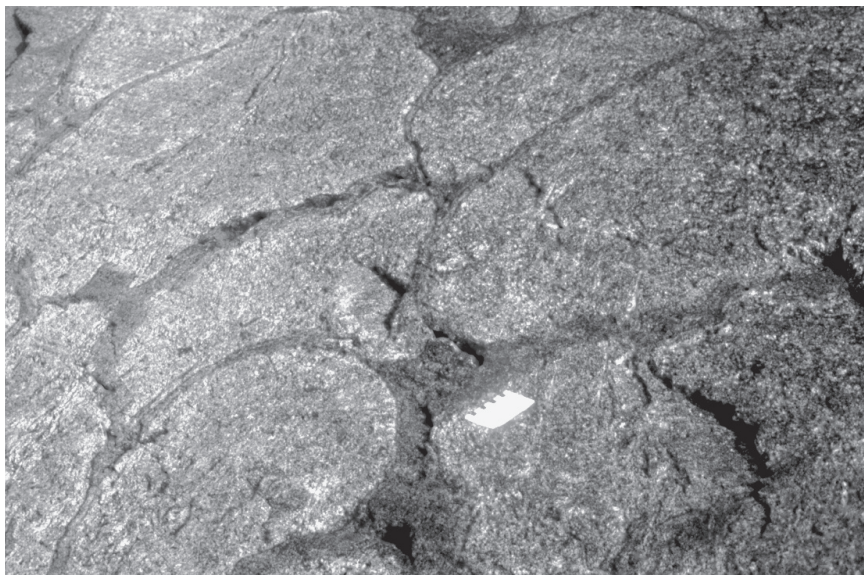


**Figure 22:** Pillowed Drumming Point andesite (unit 13a), small island north of Black Island.

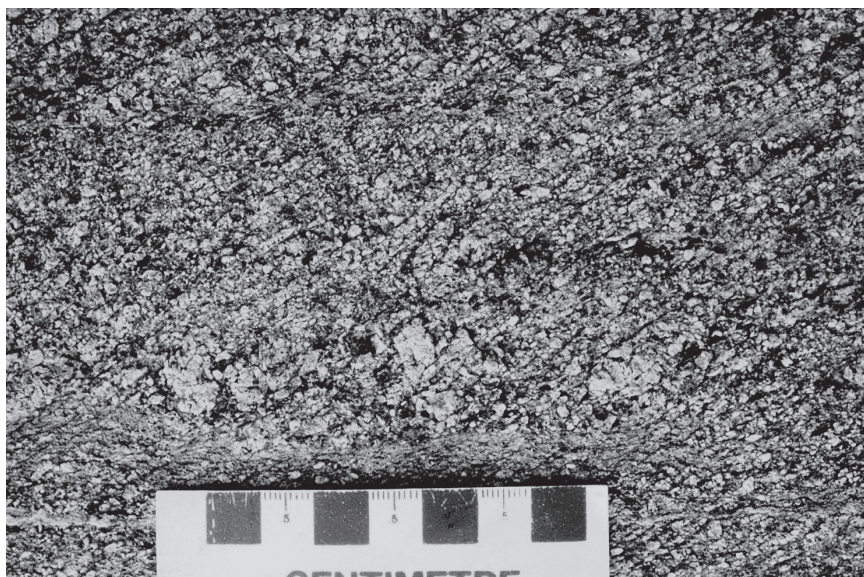


**Figure 23:** Coarse greywacke (unit 14b) with angular lithic fragments, Drumming Point sequence, northeast shore of Black Island.

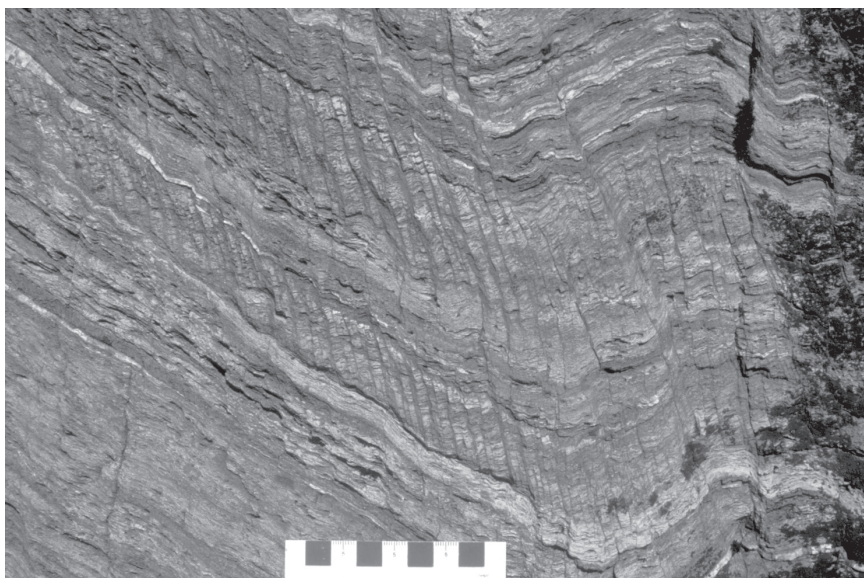


**Figure 24:** Delicately laminated siltstone and mudstone (unit 14c) folded by  $F_2$ , Drumming Point sequence, northeast shore of Black Island.



(subunit 14b) are typically massive, without discernible layering or bedding. Subunit 14b does, however, display local bedding and rare normal size-grading, attesting to its clastic character. Feldspar crystal-rich wacke (unit 14b) is texturally immature and likely represents rapid deposition of detritus locally derived from Drumming Point andesite volcanoes. A decrease in grain size from northern exposures of coarser, feldspathic volcanoclastic rocks (subunit 14b) to southern exposures of finer grained, bedded, feldspathic wacke (subunit 14a) suggests that rocks to the north may have been more proximal deposits.

Mafic mudstone (subunit 14d) outcrops on two small islands at the stratigraphic top of the exposed Black Island assemblage. The mudstone is dark grey-green on both weathered and fresh surfaces with a well-developed fissility. The mudstone may indicate that unit 14 is upward fining, but this is very speculative because of the wide spacing of exposures.

### Other rocks of the Black Island assemblage

#### *Rhyolite tuff, lapilli tuff, breccia and rhyolite cobble conglomerate (unit 15)*

Rhyolite tuff–lapilli tuff (subunit 14a) and heterolithic felsic breccia (subunit 15b) are exposed on a single outcrop on the south shore of Black Island. An imprecise U–Pb zircon age of approximately  $2732 \pm 10$  Ma for unit 15 (Ermanovics and Wanless, 1983) indicates it to be the oldest Neoarchean rock dated in the Black Island area and possibly older than the adjacent, north- and northeast-facing Point Gray basalt (unit 10), from which it is separated by an east-trending fault.

Rhyolite tuff–lapilli tuff (subunit 15a), which forms the north side of the single outcrop of unit 15, is light grey to light buff-grey on weathered surfaces and pale grey on fresh surfaces. This unit of aphyric, nonbedded, massive rhyolite breccia, which is greater than 5 m thick, comprises mainly a mixture of pale to medium grey-weathering, angular, fine-grained (glassy?) clasts and red-brown-weathering, subrounded, finely vesicular aphyric clasts. The presence in this mainly monolithic rhyolite breccia of possible shards and

flattened pumiceous clasts indicates that it may have been a pyroclastic or secondary (resedimented) pyroclastic deposit. Both the rhyolite lapilli and vesicular blocks display delicate apophyses (Figure 25), inconsistent with derivation by erosion and subaerial transport and favouring a pyroclastic origin.

Rhyolite cobble conglomerate (subunit 15b), which forms the south side of the outcrop, is well bedded and composed of a heterolithic mixture of subangular to rounded, matrix-supported felsic clasts. Beds vary in thickness from 30 to >100 cm, and one displays well-defined normal size-grading of both matrix and larger clasts (Figure 26). A block of rhyolite tuff breccia in this conglomerate contains shards and welded pumice clasts (Figure 27), suggesting that at least part of the source volcanic terrane may have been subaerial. Rounded clasts and a heterolithic clast population are consistent with subaerial transport and mixing.

#### *Gabbro and quartz diorite (unit 16)*

This unit is exposed on a number of small islands to the south and east of Deer Island. Krogh et al. (1974) reported an imprecise U–Pb zircon age of approximately  $2715 \pm 10$  Ma on a quartz diorite from this unit. The diorite and quartz diorite form fine- to medium-grained, multiphase intrusions (dike complexes) that are overprinted by a weak ( $S_1$ ) foliation. Chilled margins and rare quartz amygdules in some dikes suggest intrusion at shallow levels and possible subvolcanic character. Two gabbro samples from unit 16 have chemical signatures identical to those of the Drumming Point basaltic andesite and andesite (unit 13).

#### *Sedimentary sequences of 2.71 Ga age*

Amalgamation of disparate components of the Superior Province into a major Archean craton during the ca. 2.7 Ga Uchian orogeny was accompanied by formation of sedimentary sequences along and overlapping the resultant tectonic boundaries (Percival et al., 2002). These sedimentary successions are typically around 2.71–2.70 Ga in age. Two such successions are

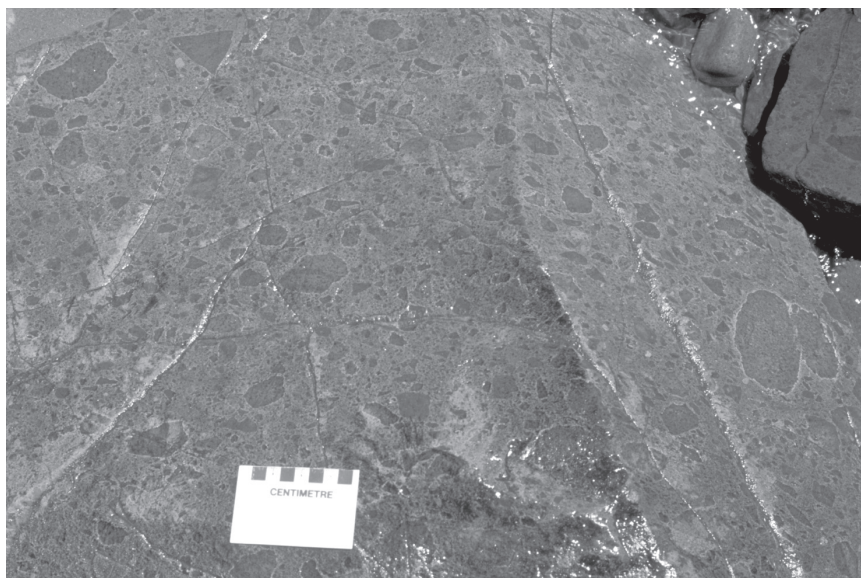


**Figure 25:** Delicate apophyses on blocks in lapilli tuff-breccia (subunit 15a), south shore of Black Island.

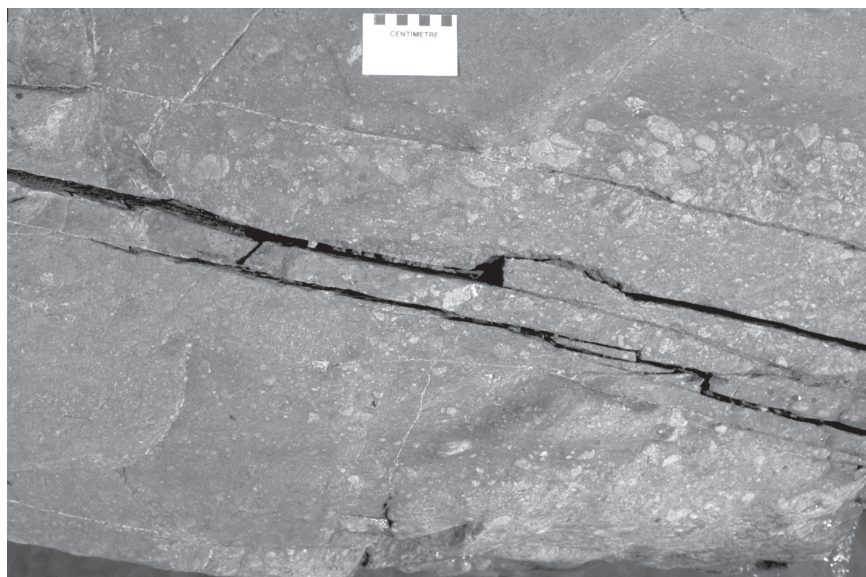


**Figure 26:** Reverse size-grading in rhyolite pebble conglomerate (subunit 15b), south shore of Black Island.

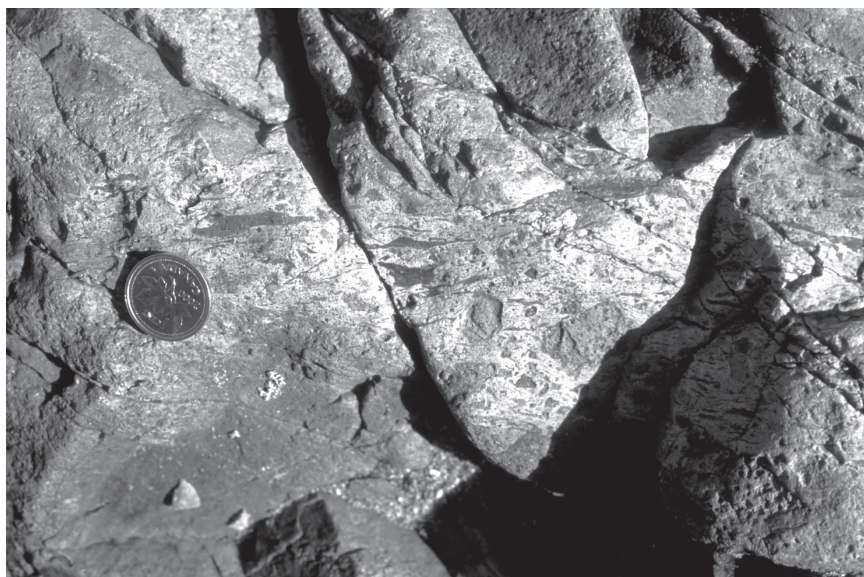


**Figure 27:** Rhyolite fragment in subunit 15b, containing flattened pumice and shards, south shore of Black Island.

present in the Black Island area. The older (<2722 Ma) Guano Island sequence forms a northwest-trending domain parallel to the  $D_1$  collisional contact between the North Caribou Terrane (units 1 and 2) and the Black Island assemblage (units 10 to 16). The younger (<2707 Ma) Hole River sequence occupies an easterly-trending domain parallel to the east-trending, dextral,  $D_3$  Seymourville Shear Zone.

#### **Guano Island sedimentary rocks**

A lens of Guano Island arkose and conglomerate <300 m wide separates the Lewis-Storey and Black Island assemblages. Contacts are not exposed because the Guano Island rocks outcrop on small isolated islands between Black Island and the east shore of Lake Winnipeg. All three subunits of unit 17 exhibit prominent  $D_1$  structures. Detrital zircons from a Guano Island arkose (unit 17b), analyzed by SHRIMP, indicate source ages between 3.0 and 2.72 Ga (Percival et al., work in progress 2005). The youngest detrital zircon age, 2722 Ma,

provides an estimate of the maximum depositional age for the unit. The Guano Island sedimentary rocks are interpreted to be syn- $D_1$  and to have formed as an overlap sequence in the collisional zone between the 3.0 Ga North Caribou Terrane and the 2.72 Ga Black Island assemblage, possibly deposited in a strike-slip basin.

#### ***Boulder conglomerate (subunit 17a)***

This unit, exposed only on Guano Island, comprises cobble- to pebble-sized clasts (Figure 28) of granitoid and volcanic rocks, vein quartz and gabbro. A  $D_1$  strain gradient is evident from the variable preservation state of clasts. On the eastern side of the outcrop, stretched pebbles in conglomerate define a prominent  $S_1$  shape fabric, which is folded into northwest-plunging  $F_1$  'Z' folds. Southwest-trending  $F_2$  folds, which locally warp of the  $S_1$  foliation and  $F_1$  folds, are particularly evident on the western slope of the island.



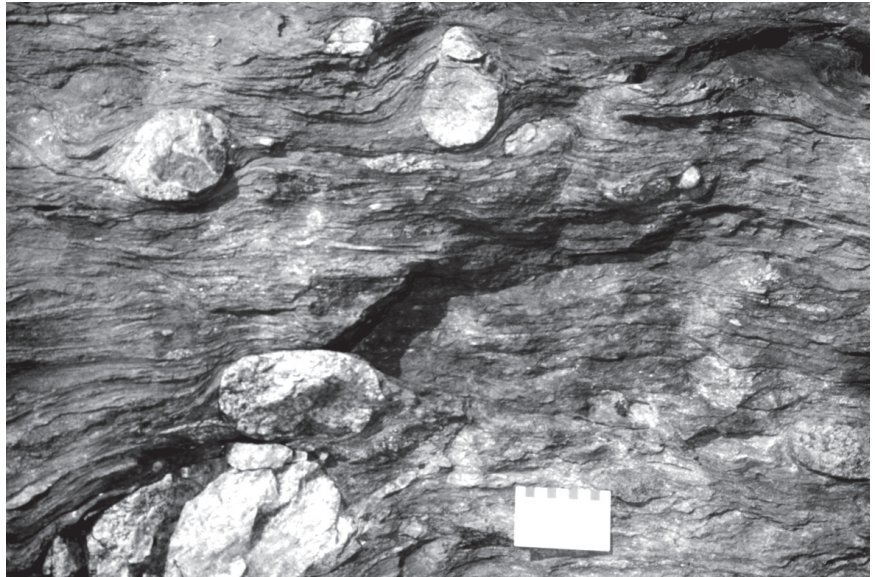


**Figure 28:** Guano Island conglomerate (unit 17a) with rounded granitic cobble, on small island between Black Island and east shore of Lake Winnipeg. Note prominent  $S_1$  schistosity and  $S_1$  flattened fragments.

#### **Arkose (subunits 17b and c)**

This unit, which is exposed on larger islands to the east of Guano Island, consists of grey massive arkose that displays a prominent north-northwest-trending, steeply dipping  $S_1$  foliation. Isolated flattened pebbles (Figure 29) are locally present in this otherwise massive uniform arkose. Bedding, if present, is strongly transposed in  $S_1$ .

#### **Hole River sedimentary rocks**

The high degree of preservation of primary sedimentary structures and presence of only weakly developed  $D_1$  structures (compared to prominent  $D_1$  structures in the Guano Island sedimentary rocks [unit 17]) may indicate the rocks to be the result of a younger, possibly late- $D_1$  episode of sedimentation. Alternatively, they may simply have been outside a prominent  $D_1$  shear-zone corridor. Consistent with the first interpretation, however, is the fact that Hole River arkose contains detrital zircons as young as 2707 Ma (Percival et al., 2000, work in progress 2005). The Hole River sedimentary rocks also contain

a range of detrital zircon ages between 3.02 and 2.707 Ga, with peaks at 2.96, 2.85, 2.80 and 2.74–2.71 Ga. In conjunction with its sedimentological features (*see below*), the <2707 Ma depositional age suggests a late-basin (Timiskaming-type) setting.

#### **Arkose (unit 18)**

Buff-weathering arkose (unit 18) in a 3.5 by 1 km east-trending unit is exposed on small islands southeast of Black Island and in scattered outcrops on the south shore of Lake Winnipeg. Overturned bedding in the arkose typically trends northeast, dips moderately to steeply northwest, and tops to the southeast. The unit is truncated to the south by the east-trending  $D_3$  Seymourville Shear Zone and to the east by a north-trending  $D_1$  fault; the latter places the west-facing Lewis-Storey assemblage against east-topping exposures of the Hole River succession.

Contact relationships between the Black Island assemblage to the northwest and the Guano Island sedimentary rocks to

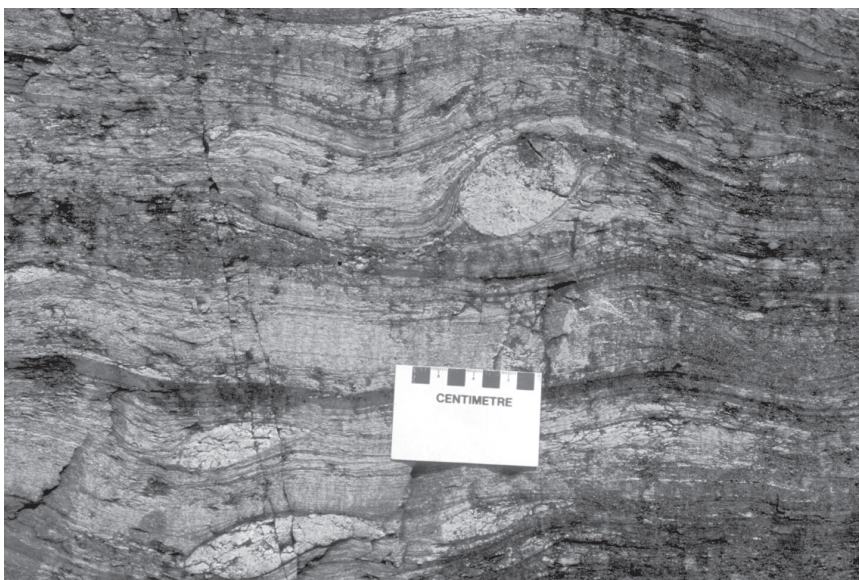


**Figure 29:** Guano Island arkose (unit 17b) with isolated,  $D_1$ -flattened, rounded granitic cobbles, on island near east shore of Lake Winnipeg.



the north are obscured by the waters of Lake Winnipeg. Their contact may be unconformable but this is difficult to establish because of the lack of exposure and the coincidence with a zone of strong  $D_3$  deformation.

The best preserved sedimentary structures in unit 18 are exposed on the islands directly north of Seymourville. Primary

structures in the arkose (unit 18) include graded bedding, pebble lags, scours and trough crossbedding (Figure 30), suggesting deposition in a subaerial-fluvial environment. East-trending  $F_3$  folds and a related  $S_3$  foliation deform the Hole River sedimentary rocks (Figure 31).

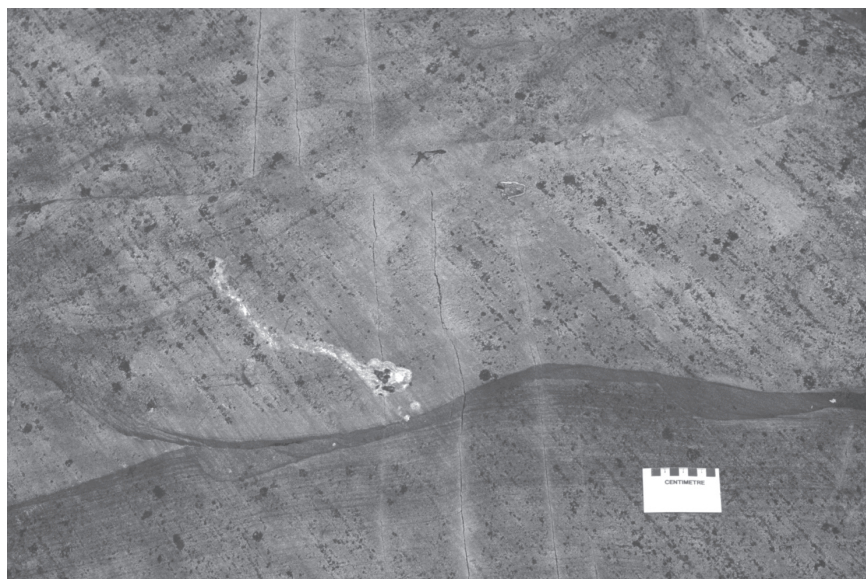


**Figure 30:** Trough crossbedded arkose (unit 18b), Hole River sedimentary rocks, on island due east of Adam Island.

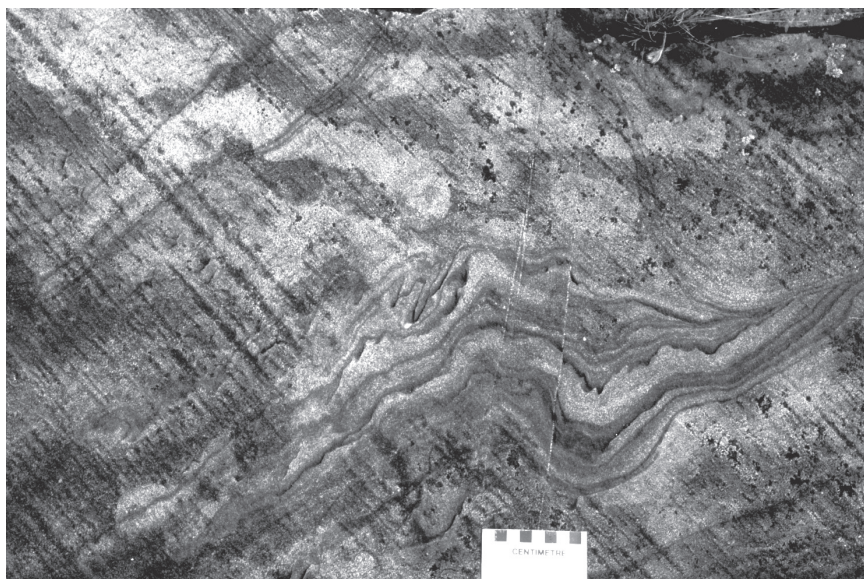


**Figure 31:** Trough crossbedded arkose (unit 18b) folded by  $F_3$ , Hole River sedimentary rocks, same location as Figure 30.



## Deformational events

Three discrete deformation events,  $D_1$  to  $D_3$ , accompanied by greenschist-facies metamorphism (Currie, 2001), have been recognized to affect all units on the regional scale. In addition, at least one event ( $D_0$ ) affected the North Caribou Terrane prior to  $D_1$ . Northwest-trending, pre- $D_1$  foliation and shear zones within the East Shore Plutonic Complex are cut locally by granodiorite dated at 2941 Ma in one locality. These structures are subparallel to  $S_1$  and distinguished from it by a subhorizontal stretching lineation (Percival et al., 2005). For the most part, early structures in the East Shore Plutonic Complex and Lewis-Storey assemblage are composite  $D_0$ - $D_1$  structures.

In tonalite (unit 1),  $D_0$  strain intensity varies from weak mineral alignment without associated linear fabric elements to high-strain zones recrystallized in the greenschist facies, with a prominent gently plunging rodding lineation. These zones of intense foliation and grain-size reduction range up to 8 m in width, and affect both tonalite and mafic sills. Evidence of shear strain is common in tonalite (unit 1), where chloritic folia surrounding plagioclase phenocrysts develop extensional shear bands. These textures, which become more pronounced in  $D_0$  high-strain zones, indicate mainly dextral shear (Figure 32).



**Figure 32:** Large-scale dextral shear bands in the layered sequence (unit 2), East Shore Plutonic Complex. Note boudinaged mafic sills, east shore of Lake Winnipeg.

### $D_1$ deformation

Strain associated with the  $D_1$  deformation is focused in the contact zone between the Lewis-Storey and Black Island assemblages, and generally increases in intensity from north to south. Strike direction varies in a broad arc, from northwest in the north to north-northwest in the south, with dips being consistently steep to the southwest. In the East Shore Plutonic Complex,  $D_1$  and possible pre- $D_1$  fabrics strike parallel to the shoreline and to lithological contacts.

In the layered sequence (unit 2), north-northwest-trending  $D_1$  ductile deformation zones up to 100 m wide are parallel to lithological contacts. Moderately northwest-plunging folds and rodding lineations are common, particularly in high-strain zones. Kinematic indicators include prominent 'Z' folds and extensional shear bands. A pervasive, composite, grain-scale  $S_0$ - $S_1$  foliation is evident in sedimentary units of the Lewis-Storey assemblage (units 3 to 7), as well as in talc schist and serpentinite derived from komatiitic rocks. Arkosic grit (unit 3) commonly develops extensional shear bands, indicating dextral shear (Figure 6).

North-northwest-striking  $D_1$  high-strain zones up to 300 m wide dissect units of the Black Island assemblage, separated by weakly foliated zones that retain primary structures. Most zones occur within lithological units, rather than at major contacts. At low strain levels, the foliation in shear zones can be traced to attenuated pillow selvages, whereas higher strains develop a millimetre-scale tectonic lamination. In their most deformed state,  $D_1$  mafic tectonite (units 10b and 13d) develops 1) discrete zones of laminated carbonate-chlorite-quartz schist, commonly crenulated in younger deformation events (Figure 14); and 2) 'younger' folds that can locally be demonstrated to be due to progressive fold development during incremental  $D_1$  strain (Figure 33).

The Guano Island sedimentary sequence carries prominent  $D_1$  fabrics. In the arkose units (unit 17c, d), pervasive, intense bedding-parallel foliation and associated gently south-plunging rodding lineation indicate high levels of strain, as does a fine-scale  $D_1$  tectonic lamination and isoclinal  $F_1$  folds (Figure 34) developed in conglomerate (unit 17a, b).

In contrast,  $D_1$  fabrics appear weak or absent in the Hole River sequence (unit 18), where folds of bedding are accompanied by an  $S_3$  axial-planar foliation. Only locally can a weak bedding-parallel fabric be discerned. This is in contrast to the on-strike north-trending  $D_1$  shear zones to the north. This indicates that either the Hole River sequence is a late  $D_1$  cover sequence or that the  $D_1$  shear zones are offset by younger ( $D_2$  or  $D_3$ ) shear zones, or a combination of both.

### $D_2$ deformation

The  $D_2$  deformation is expressed sporadically throughout the area as open folds and crenulations in fissile zones and weak axial-planar foliation. The  $S_2$  foliation strikes southwesterly, with subvertical dips;  $F_2$  fold hinges plunge gently southwest, reflecting intersection with southwest-dipping  $S_1$  planes.



**Figure 33:** Z-shaped  $F_1$  folds transected by  $S_1$  foliation, suggesting progressive fold development during incremental  $D_1$  strain in a  $D_1$  shear zone in Gray Point basalt (unit 10b), Gray Point.

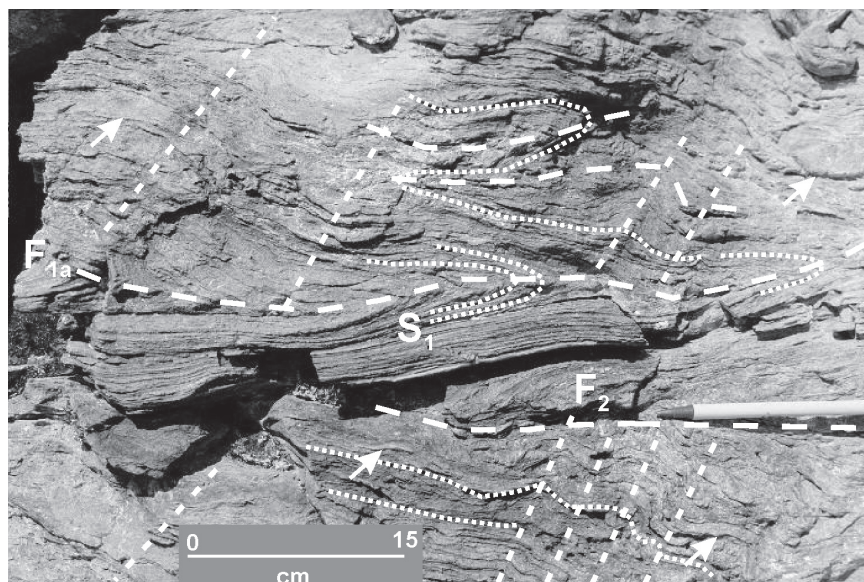
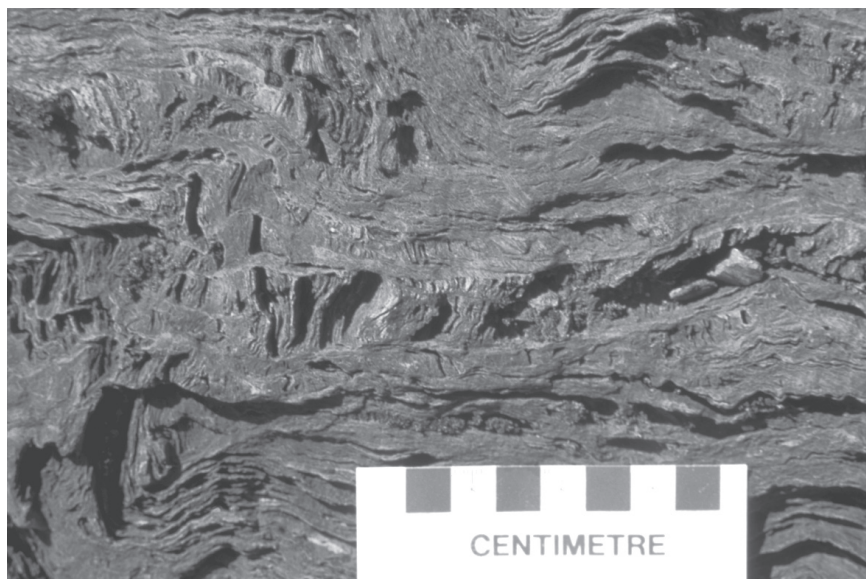


**Figure 34:** Stretched-pebble conglomerate (flattened clasts indicated by arrows) of the Guano Island sequence, showing strong  $S_1$  tectonic lamination, tight  $F_1$  Z-folds and open  $F_2$  crenulations, on an island between Black Island and the east shore of Lake Winnipeg.

The intensity of  $D_2$  strain appears weak to modest throughout most of the area; however, in the southernmost exposures of the Black Island sequence,  $D_2$  shear zones overprinting  $S_1$  fabrics may have accommodated significant transcurrent displacement (Figure 35).

On islands north of Seymourville, tight  $F_2$  chevron folds occur at the boundaries of a 10 m wide  $D_2$  shear zone. Outcrop observations indicate that the dextral shear fabric developed through transposition of  $S_1$  foliation along  $F_2$  fold limbs. These islands are separated by water from exposures of Hole River arkose to the south that lack evidence of penetrative  $D_1$  deformation.

### **$D_3$ deformation**

Strain associated with the  $D_3$  deformation is most evident in the 1 km wide, east-trending, steeply dipping Seymourville Shear Zone, which marks the southern limit of the Hole River sedimentary sequence and accommodated approximately 7 km

of dextral offset of the basal Lewis-Storey unconformity.

Overprinting relationships between the chlorite-grade  $D_3$  shear structures and older fabrics are evident at many locations within and adjacent to the Seymourville Shear Zone. In the southeast corner of the map area, northwest-trending  $D_1$  shear zones can be traced into westerly trends through a zone of  $F_3$  crenulation. Within the shear zone, pods of quartz-carbonate-chlorite schist, characteristic of  $D_1$  shear zones, display isoclinal  $F_3$  'Z' folds of  $S_1$  layering (Figure 36). Near the southern margin of the zone, tonalite with northeast-trending  $S_2$  foliation is transected by  $D_3$  shear zones showing dextral deflection.

Although part of the linear nature of the zone results from reorientation of older structures, a significant component is an  $S_3$  shear fabric. This penetrative foliation and associated green-schist-facies protomylonite and mylonite zones dip steeply south ( $70-85^\circ$ ) and are accompanied at high strain levels by a subhorizontal stretching lineation. A steep  $S_3$  cleavage and associated  $F_3$  folds are the dominant fabrics in the southern half



**Figure 35:** Chlorite-carbonate-quartz schist developed in  $D_1$  shear zone (unit 10b) on Gray Point. Note minor  $F_1$  fold in lower left corner and  $F_2$  crenulations.

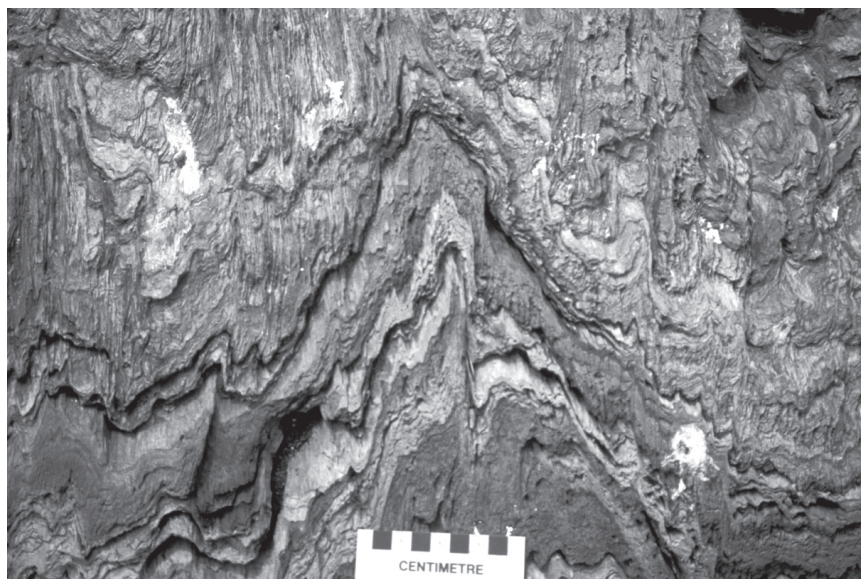
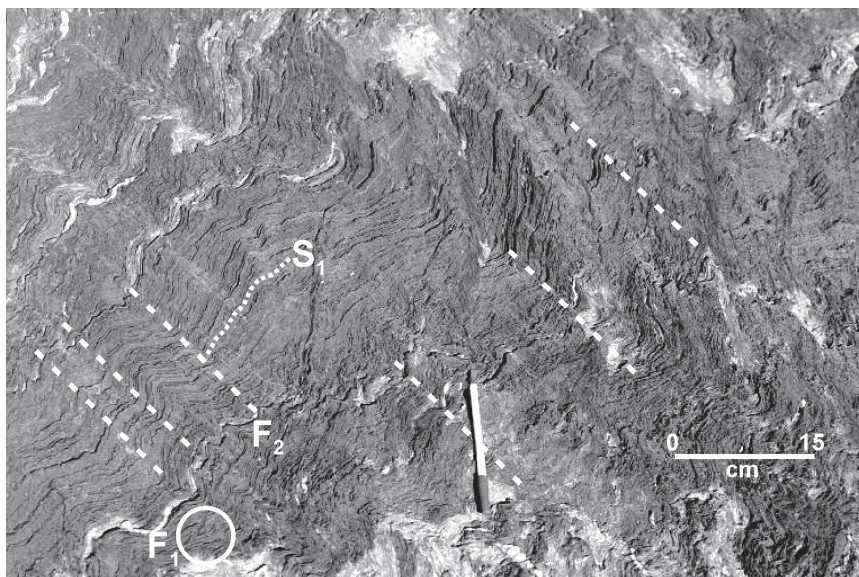


**Figure 36:**  $F_3$  crenulation and folding of  $D_1$  shear zone (unit 10b) on the small island directly north-west of Adams Island. In less highly strained domains on the island, the  $S_1$  fabric can be clearly demonstrated to have developed from pillowed basalt of the Gray Point sequence.

of the Hole River sedimentary section.

The poorly exposed region south of the Seymourville Shear Zone consists mainly of tonalitic rocks (Ermanovics, 1981). Observations of structures and overprinting relationships

permit definition of several structural domains characterized by dominant  $D_1$  and  $D_2$  structures. Additional regional structural elements not present north of the Seymourville Shear Zone, however, appear necessary to explain the structural geometry.

## Geochemistry of Black Island assemblage volcanic rocks

Least altered samples were collected from all major volcanic units in the Black Island assemblage. Samples were trimmed to remove fractures, veins and weathered surfaces, and to avoid visible alteration or significant amygdale populations. Fourteen volcanic rocks from the Black Island assemblage were submitted for high-precision inductively coupled plasma-mass spectrometry (ICP-MS) geochemical analysis and six for Nd-Sm isotopic analysis. The ICP-MS and Nd-Sm analyses were done at Activation Laboratories Ltd. and Memorial University, respectively. Information on analytical techniques is included on the 'Readme' worksheet in Data Repository item DRI2005004. The trace-element, rare-earth-element and Sm-Nd geochemistry have been used to identify the most likely tectonomagmatic environment of formation for Black Island assemblage volcanic rocks and to guide their possible correlation to units elsewhere in the Rice Lake belt.

Major-element and immobile trace-element discrimination plots indicate that the Gray Point sequence (Figure 37a, c) is composed of basalt and basaltic andesite (46–54% SiO<sub>2</sub>), whereas the Drumming Point sequence (Figure 37b, d) is slightly more felsic and composed of basaltic andesite and andesite (55–63% SiO<sub>2</sub>). Both sequences are subalkaline (Figure 37).

### Mafic volcanic rocks

Gray Point basalt and basaltic andesite display many of the geochemical characteristics of ocean-floor basalt. They fall in the field of modern ocean-floor basalt on a plot of Cr vs. Ti (Figure 38a) and in the field of tholeiitic basalt on a Jensen cation plot (Al<sub>2</sub>O<sub>3</sub> vs. FeO<sub>tot</sub>+TiO<sub>2</sub> vs. MgO; Figure 38c). On diagrams using Th values or Th/Nb ratios (e.g., Figures 38e, 39a, b), they plot within the arc field, slightly outside the ocean floor-normal mid-ocean ridge basalt (N-MORB) field. Multi-element N-MORB- and primitive-mantle-normalized plots (Figure 40a) show that the basalt has elevated Th and slightly negative Nb values, but typical N-MORB geochemical characteristics in all other respects, including light rare-earth element (LREE) depletion.

The elevated Th/Nb of Gray Point basalt could be a result of crustal contamination, a minor subduction component or fractionation processes in an oceanic-plateau setting (e.g., Mamberti et al., 2004). None of these processes, however, satisfactorily explains the geochemical signatures displayed by these rocks. For example, their positive epsilon Nd ( $\epsilon_{Nd}$ ) values (Figure 41) indicate them to be isotopically juvenile and unlikely to have involved crustal contamination. The

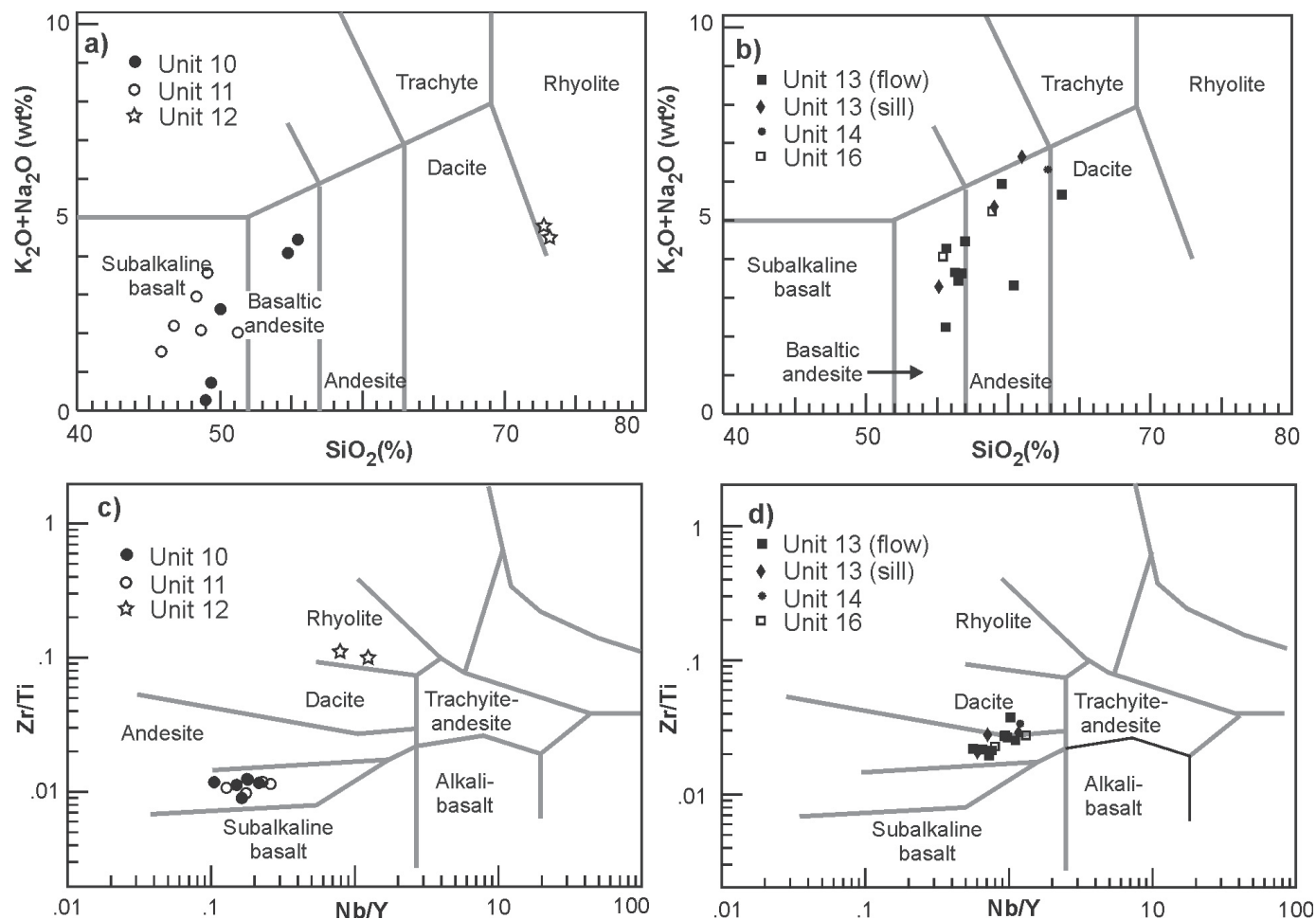


**Figure 37:** Black Island assemblage volcanic rocks plotted on geochemical discrimination plots for rock type and major chemical affinities: a), b) SiO<sub>2</sub> vs. K<sub>2</sub>O+Na<sub>2</sub>O (LeMaitre et al., 1989); and c), d) Nb/Y vs. Zr/Ti (Winchester and Floyd, 1977).

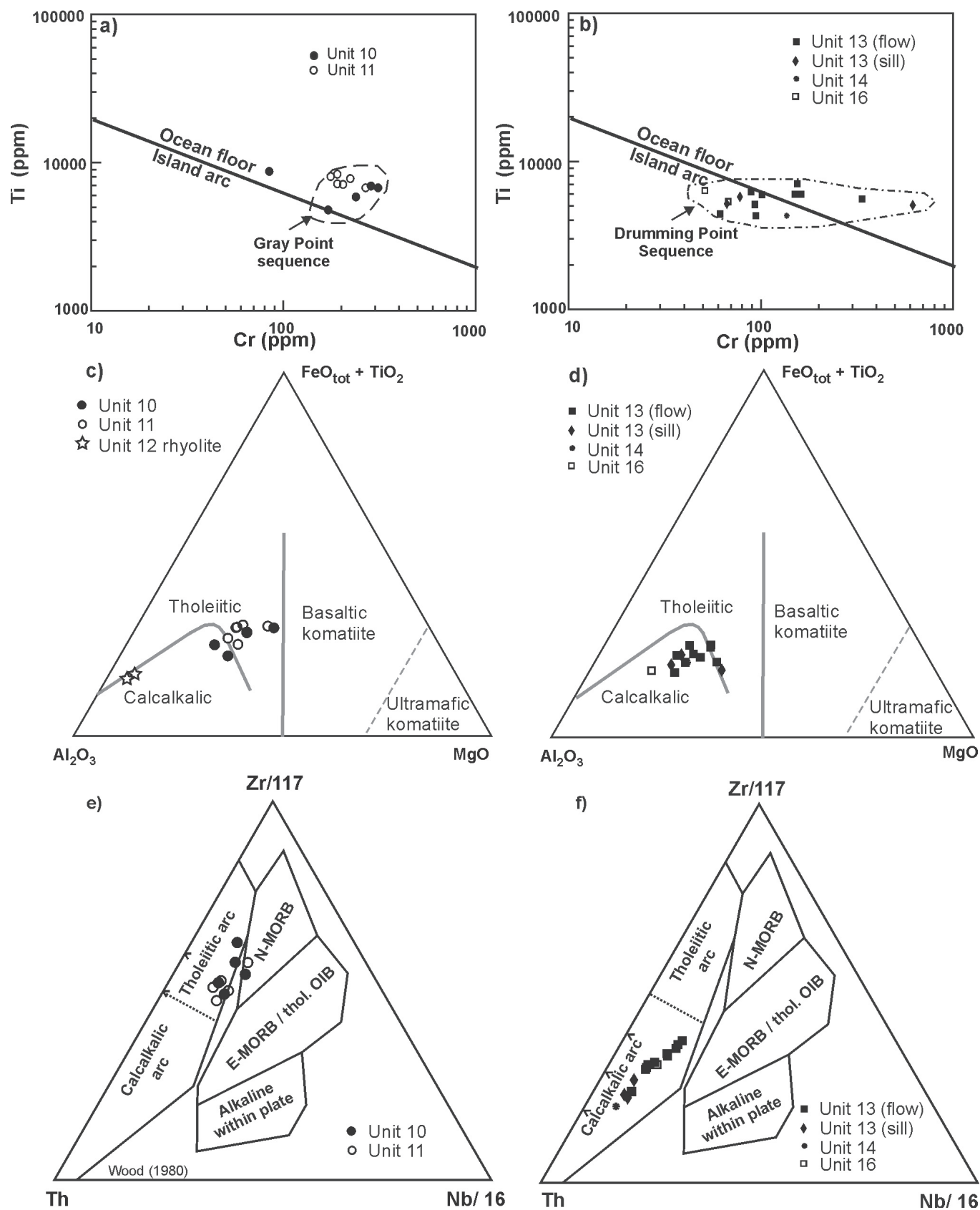


**Figure 38:** Black Island assemblage basalt, basaltic andesite and andesite plotted on major- and trace-element discrimination diagrams: **a), b)** Cr vs. Ti (Pearce, 1975); **c), d)** Jensen cation ( $\text{Al}_2\text{O}_3$  vs.  $\text{FeO}_{\text{tot}} + \text{TiO}_2$  vs.  $\text{MgO}$ ; Jensen, 1976); and **e), f)** Th vs. Zr/117 vs. Nb/16 (Wood, 1980). Abbreviations: E-MORB, enriched mid-ocean ridge basalt; N-MORB, normal mid-ocean ridge basalt; OIB, oceanic-island basalt.



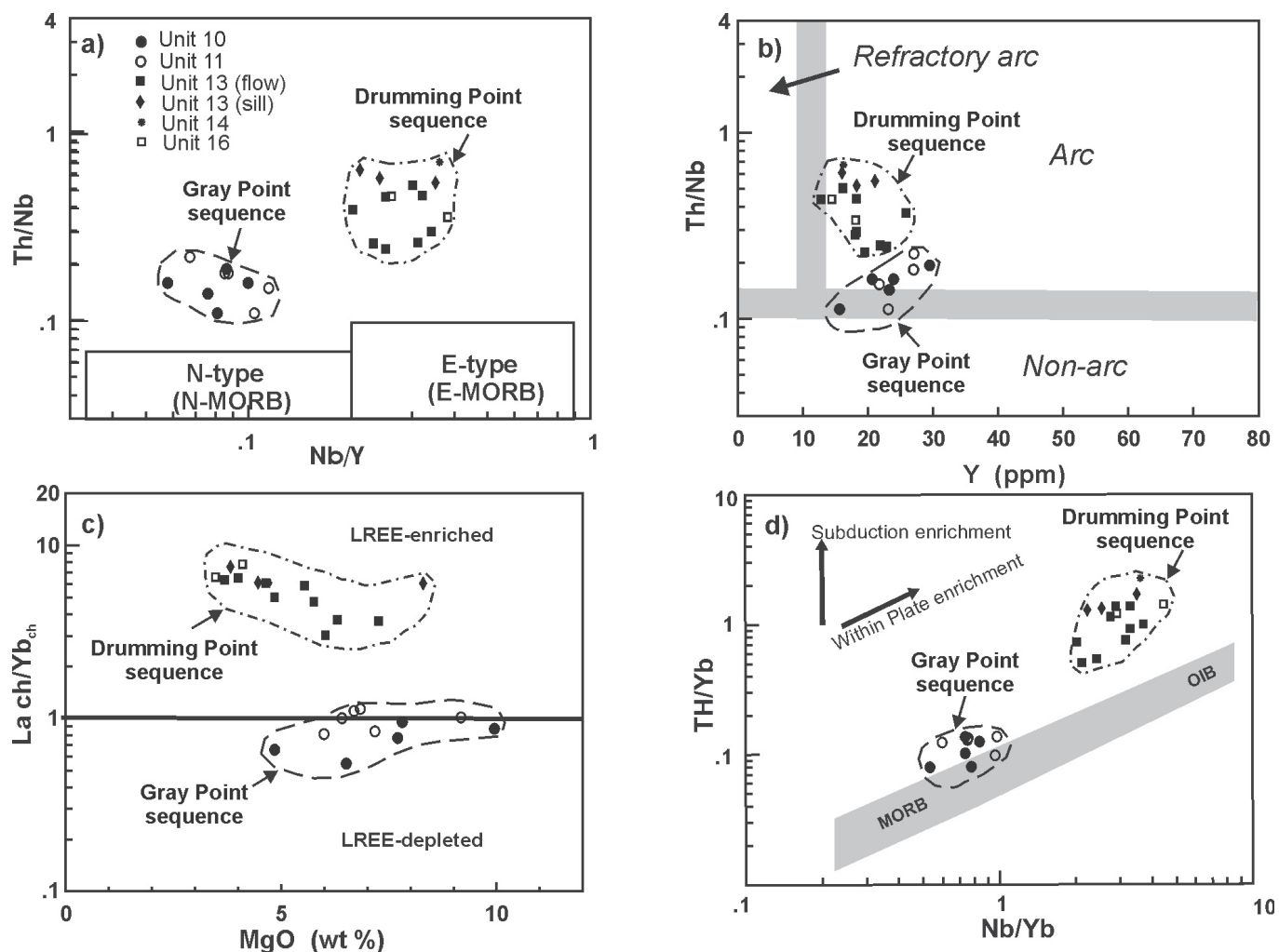


**Figure 39:** Black Island assemblage volcanic rocks plotted on various geochemical discrimination diagrams: **a)** Nb/Y vs. Th/Nb (Pearce, 1983; Swinden, 1996); **b)** Y vs. Th/Nb; **c)** MgO vs.  $La_{ch}/Yb_{ch}$  (Stern et al., 1995); and **d)** Nb/Yb vs. Th/Yb (Stern et al., 1995). Abbreviations: E-MORB, enriched mid-ocean ridge basalt; LREE, light rare-earth element; N-MORB, normal mid-ocean ridge basalt.

absence of negative Zr, Hf and Ti anomalies is not consistent with genesis in a subduction or arc environment. Their position outside the within-plate (oceanic-island basalt (OIB)–plume) field on discriminant plots recommended by Pearce (1996) for distinguishing between ocean-floor and within-plate (plume) basalts (Figure 42) does not support an oceanic-plateau origin. However, basalt geochemically similar to that in the Gray Point sequence is present in modern back-arc environments (Gribble et al., 1996; Saunders et al., 1991) and in the Paleoproterozoic Flin Flon Belt (Stern et al., 1995). Both the modern (Stopler and Newman, 1994; Gribble et al., 1996) and the Paleoproterozoic (Stern et al., 1995) basalts are interpreted to be ocean-floor–back-arc basalt that has been modified by hydrous fluxing of the upwelling MORB-source asthenosphere. Stern et al. (1995) suggested that the arc signature in the Paleoproterozoic ocean-floor basalt at Flin Flon was acquired by mixing of upwelling MORB-source asthenosphere with metasomatized (hydrated) arc-mantle lithosphere (e.g., Sinton and Fryer, 1987).

On primitive-mantle–normalized multi-element plots, the Gray Point basalt (Figure 40a) is geochemically similar to the

Unnamed, Tinney and Gunnar basalt units (Figure 40b) of the eastern Rice Lake greenstone belt. The latter units outcrop 80 km to the east, where they form a basaltic ‘platform’ at the base of the Bidou Lake subgroup. However, the basaltic units in the Rice Lake belt are >2.733 Ga and therefore at least 10 m.y. older than the Gray Point basalt.

The Drumming Point basaltic andesite and andesite straddle the ocean-floor and island-arc fields of modern volcanic rocks on the Cr vs. Ti plot (Figure 38b). They show an arc signature on all discriminant plots shown in Figure 39 and fall in the calcalkaline field on the Jensen cation plot (Figure 38d) and the Th, Zr and Nb plot (Figure 38e). Elevated light rare-earth elements (LREE) and depleted heavy rare-earth elements (HREE) on the N-MORB– and primitive-mantle–normalized multi-element plots (Figure 40) are consistent with a calcalkalic affinity for the Drumming Point sequence. On multi-element N-MORB–normalized (Figure 40) plots, the Drumming Point sequence displays negative Nb anomalies relative to Th, La and Ce, a feature that is typically attributed to subduction processes in modern volcanic regimes (Pearce and Peate, 1995). However,

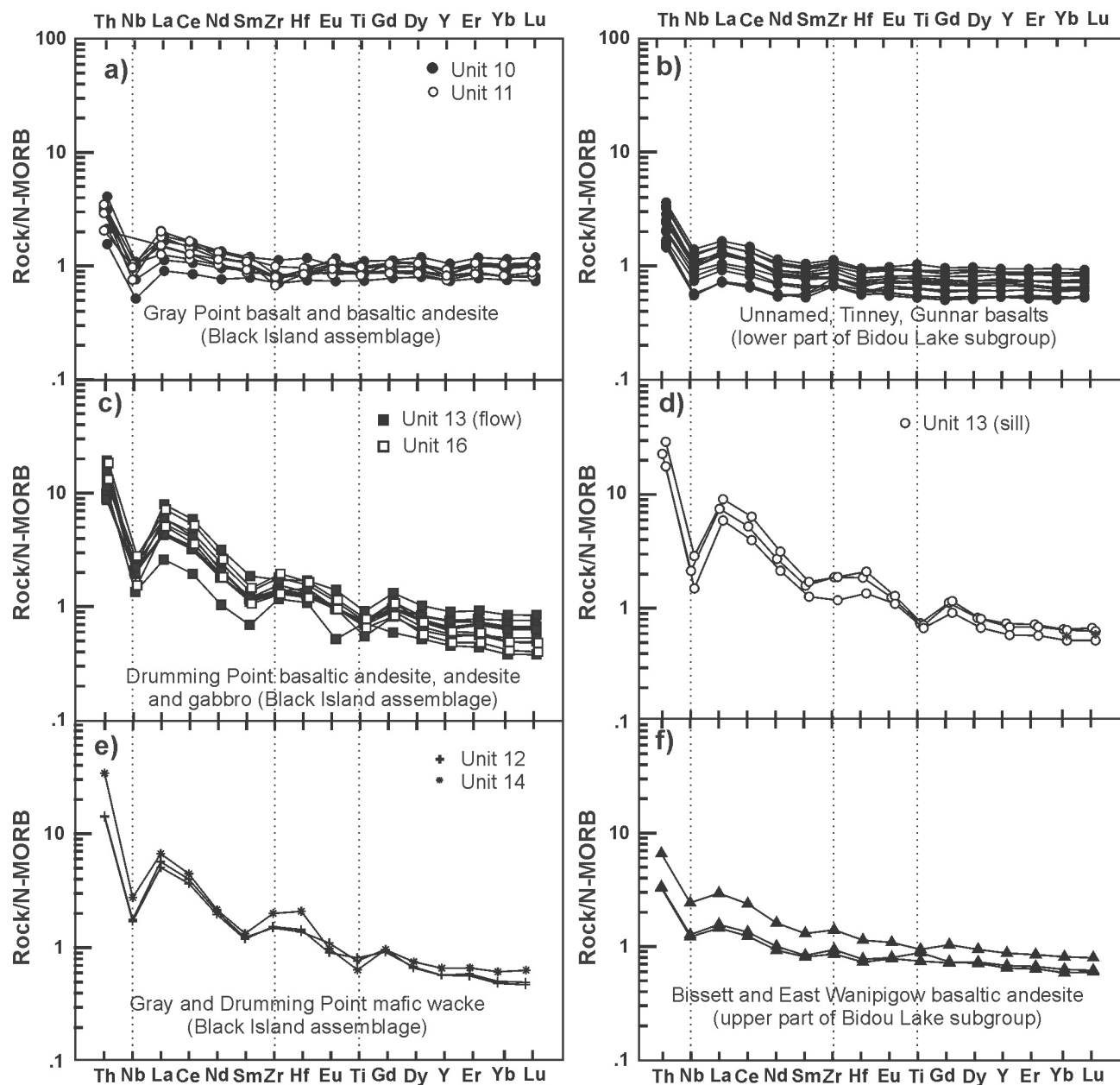


**Figure 40:** Multi-element plots of Black Island assemblage and Bidou Lake subgroup mafic volcanic rocks normalized to normal mid-ocean ridge basalt (N-MORB). Normalizing values and order adopted from Stern et al. (1995).

Zr and Hf do not show troughs on these plots that are typical of magmas in modern arc environments. Negative  $\epsilon_{\text{Nd}}$  values (Figure 41) for the Drumming Point andesite strongly suggest that its genesis may have involved contamination by older crust. The Drumming Point sequence andesite is geochemically similar to mafic volcanic rocks that occur within the upper Bidou Lake subgroup at Bissett and Wanipigow Lake (Figure 40f).

The dramatic geochemical differences between the N-MORB-like Gray Point and calcalkaline Drumming Point sequences indicate that their boundary is significant. The interface, which is marked by a hiatus in mafic volcanism and the deposition of products of erosion, represents an important change in the tectonic environment of magmatism from back arc to subduction generated.

### Felsic volcanic rocks

Two samples from the  $2732 \pm 10$  Ma rocks of unit 15 fall within the volcanic-arc and syncollisional field on a Nb vs. Y plot (Figure 43) and within the arc-related field on a plot of Zr vs.  $\text{TiO}_2$  (Figure 44a). On a multi-element, primitive-mantle-normalized plot (Figure 45a), these rocks display negative Nb relative to Th, La and Ce, a feature typical of modern subduction-related volcanic rocks, and they plot within the calcalkaline field on a Th/Yb vs.  $\text{Yb}_n$  plot (Figure 44b). In all respects, they are geochemically indistinguishable from  $(2729 \pm 3.2 \text{ Ma})$ ; Turek et al., 1989) Bidou Lake subgroup felsic volcanic rocks of similar age occurring 75 km to the east at Bissett.

Two samples of clasts from rhyolite breccia, from the dominantly intermediate volcanoclastic rocks (unit 12) that

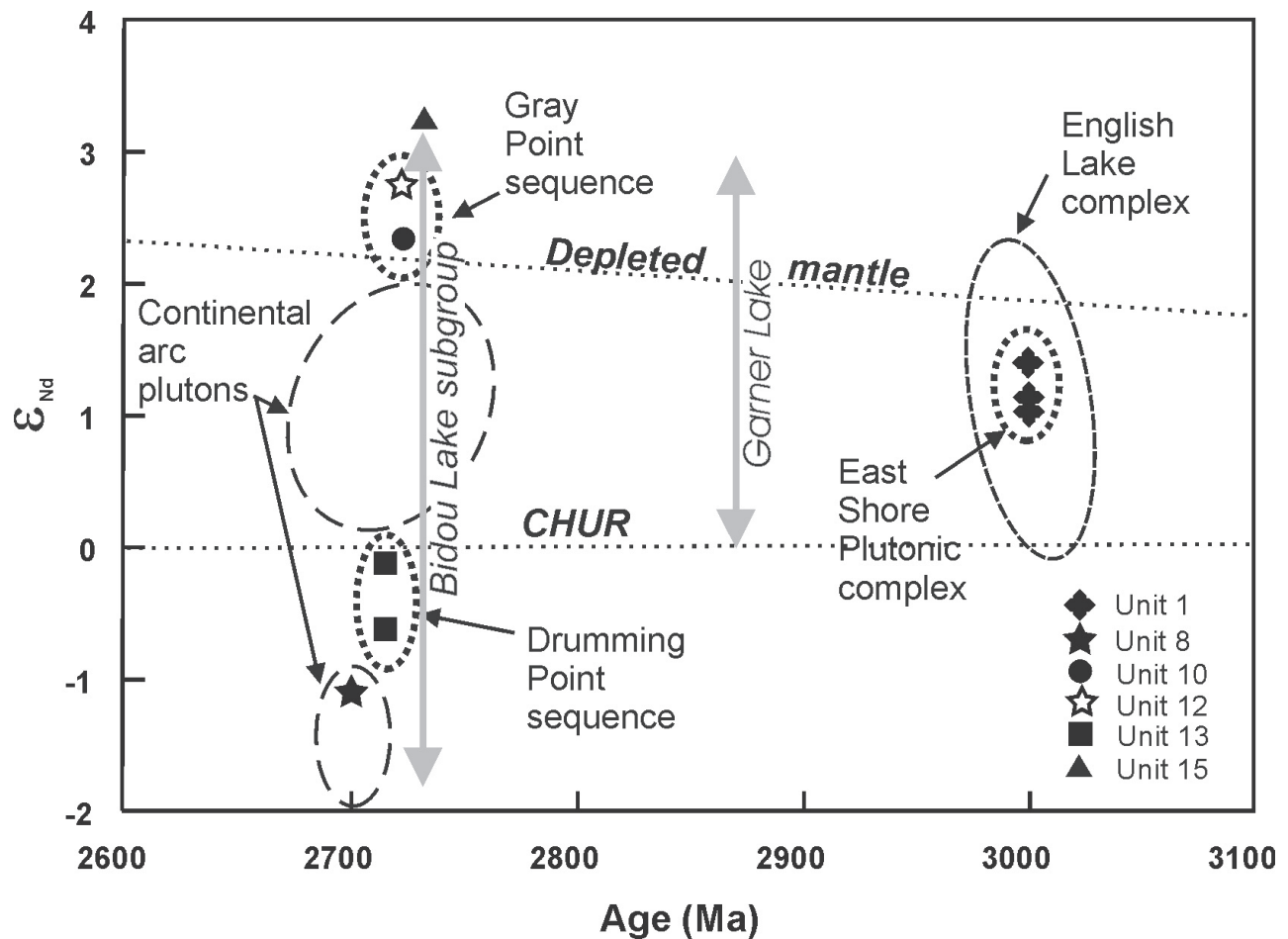


**Figure 41:** Epsilon Nd ( $\epsilon_{Nd}$ ) value versus age for volcanic rocks of the Black Island assemblage and plutonic rocks of the East Shore Plutonic Complex. The fields of the 3.0 Ga English Lake complex, the 2.8 Ga Garner Lake volcanic rocks, the 2.73 Ga Bidou Lake subgroup volcanic rocks and the 2.70–2.73 Ga continental-arc plutonic rocks are shown for comparison. The 'Depleted mantle' evolution curve is after DePaolo (1988). Abbreviation: CHUR, chondritic uniform reservoir.

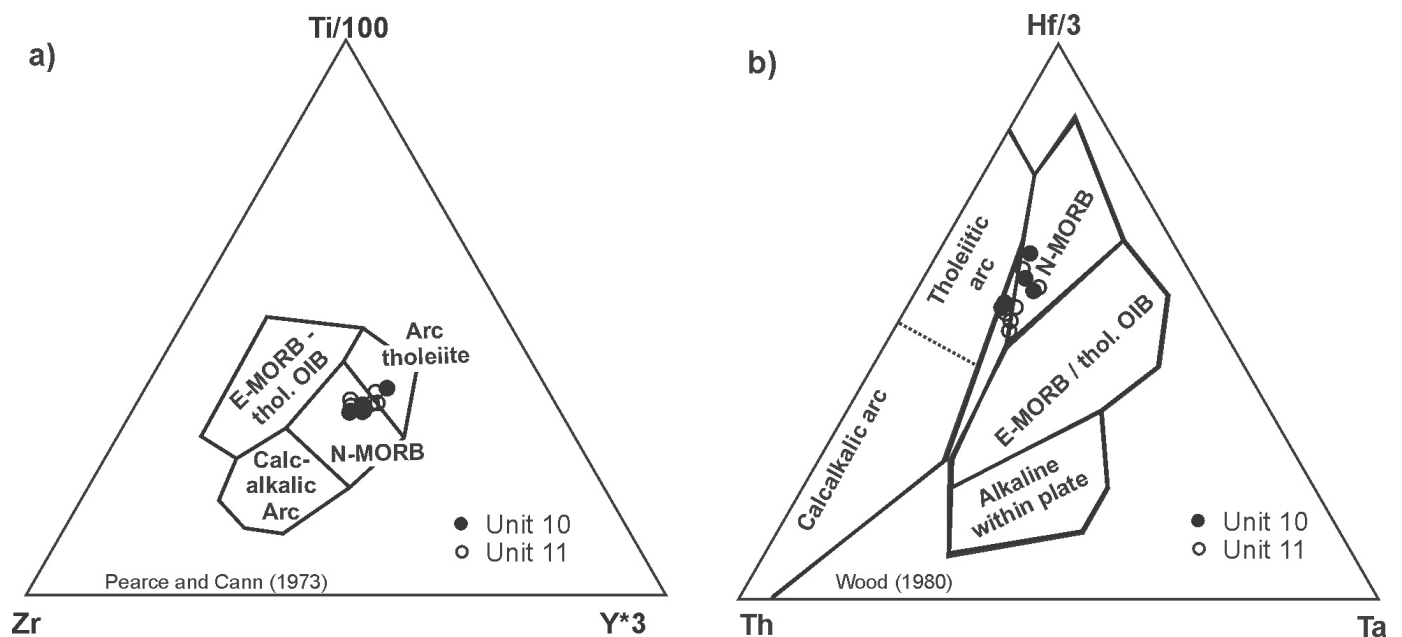


**Figure 42:** Gray Point basalt and basaltic andesite (units 10 and 11) plotted on a) Zr vs. Ti/100 vs. Y\*3 (Pearce and Cann, 1973) and b) Th vs. Hf/3 vs. Ta (Wood, 1980) discriminant diagrams.

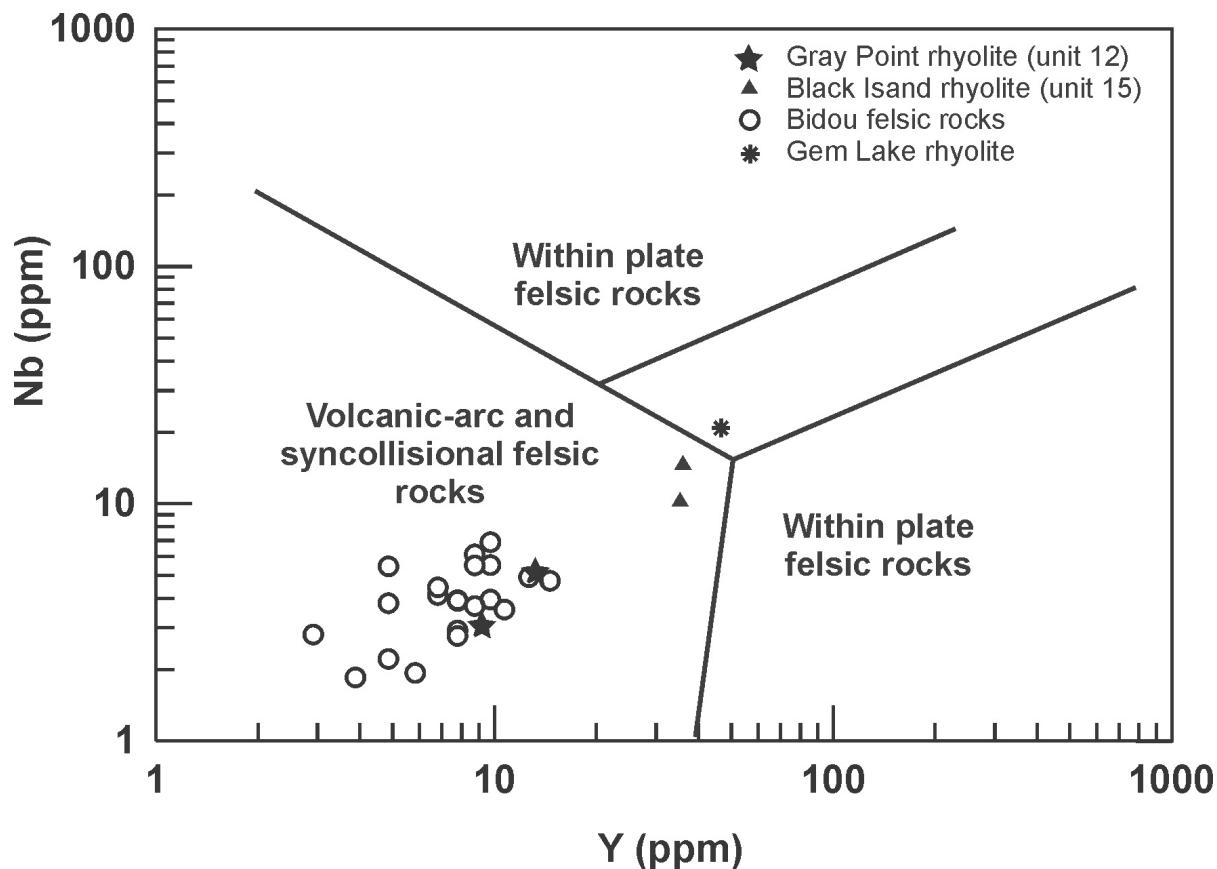


**Figure 43:** Comparison of Black Island assemblage rhyolite with those of the 2.73 Ga Bidou Lake and 2.72 Ga Gem Lake volcanic assemblages, Rice Lake greenstone belt, on a granitic-rock discriminant plot of Y vs. Nb (Pearce et al., 1984). The broken line is the field boundary for within-plate granitic rocks from anomalous ridges. Bidou and Gem Lake analyses are from DRI2005004.

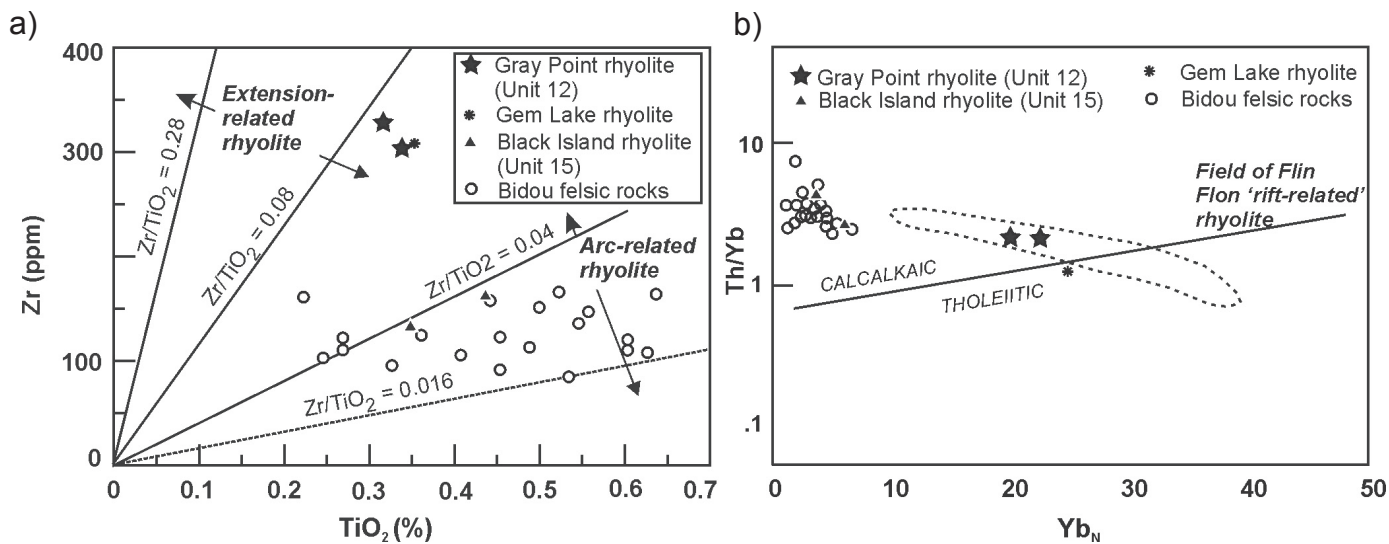


**Figure 44:** Comparison of Black Island assemblage rhyolite with those of the 2.73 Ga Bidou Lake and 2.72 Ga Gem Lake volcanic assemblages, Rice Lake greenstone belt, on plots of **a)** Zr vs.  $\text{TiO}_2$  (Barrett and MacLean, 1994; modified by Syme, 1998); and **b)** Th/Yb vs.  $\text{Yb}_N$  (Syme, 1998). Fields of extension-related and arc-related rhyolite are defined on the basis of Paleoproterozoic rhyolite from the Flin Flon area. Analyses for Bidou Lake and Gem Lake volcanic assemblages are from DRI2005004.

lie at the top of the 2723 Ma Gray Point sequence, plot within the volcanic-arc and synvolcanic field on the Nb vs. Y plot (Figure 43) but close to the boundary of 'within-plate' felsic rocks. On a plot of Th/Yb vs.  $Yb_n$  (Figure 44b), they fall in the field of 'rift-related' Flin Flon rhyolite. On multi-element, primitive-mantle-normalized plots (Figure 45b, d), they are indistinguishable from an analysis of a Gem Lake felsic volcanic rock. The proximity to the within-plate field in

Figure 43 and the similarity to rift-related rhyolite in Figure 44 suggest that this rhyolite sequence formed in an extensional regime. These characteristics are markedly different than those of the structurally underlying subduction-related 2732  $\pm$  10 Ma rhyolite (unit 15) and the younger calcalkaline rocks of the stratigraphically overlying Drumming Point sequence (units 13 and 14).

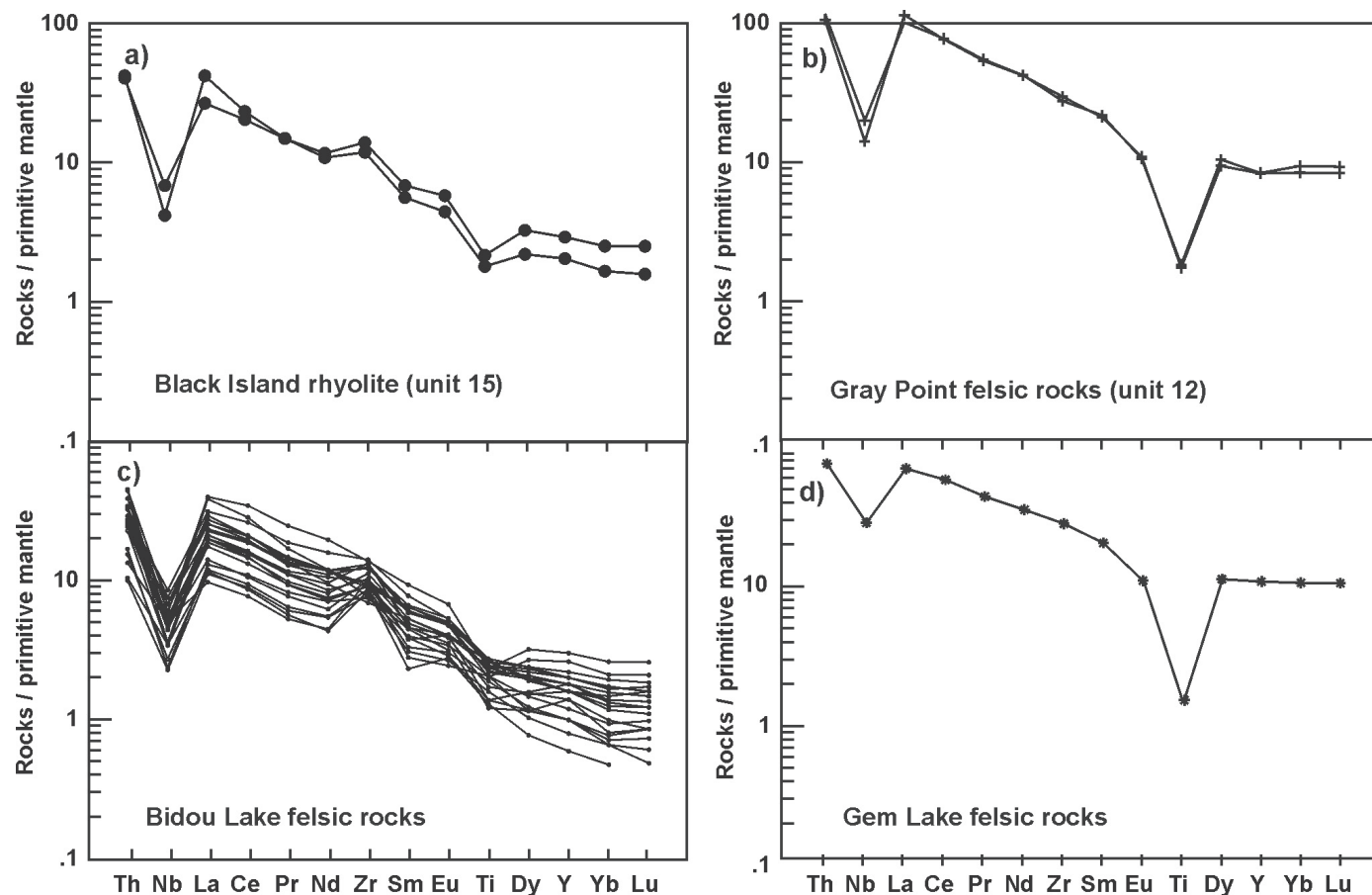


**Figure 45:** Primitive-mantle-normalized (Sun and McDonough, 1989) extended-element plots of geochemical data for felsic rocks of the Rice Lake greenstone belt: **a)** Black Island assemblage rhyolite (unit 15), **b)** Gray Point rhyolite (unit 12), **c)** Bidou Lake rhyolite (DRI2005004), and **d)** Gem Lake rhyolite (DRI2005004).



## Economic geology

The Rice Lake greenstone belt has a long history as a lode-gold producer. Shear zones and related quartz-carbonate vein stockworks, belonging to  $D_1$ , on the eastern shore of Black Island and on smaller islands display sericite and ankerite alteration. With a few exceptions, no surface exploration activity (trenches or sampling) was observed on these zones, indicating that their potential has probably not been adequately assessed. Grab samples of sulphide-bearing zones, however, yielded low Au values in the 2–63 ppb range.

The ca 3.0 Ga crust (units 1 and 2) east of Lake Winnipeg and the unconformably overlying Lewis-Storey rift-platform sedimentary rocks (units 3–7) are a previously unrecognized and largely unexplored succession. The ca. 3.0 Ga crust of the North Caribou Terrane is one that could have potential for

diamond exploration, since old Archean crust can be bonded to stable refractory mantle lithosphere that includes the diamond stability field (Richardson et al., 1984). Mafic and ultramafic rocks of the English Lake Complex, also relatively unexplored, have not yielded encouraging results for nickel or platinum group elements (PGE; Young and Theyer, 1990).

The economic potential of the Lewis-Storey rift-platform sequence is not known. Ultramafic rocks in Paleoproterozoic rift successions, such as those in the Thompson Nickel Belt and circum-Superior region, are known to host magmatic Ni and PGE. To date, however, significant Mesoproterozoic Ni and PGE deposits are not known. Ultramafic units drilled east of Black Island have combined Ni-Cu contents up to 2.1 wt.% (A.F. 93757).

## Discussion and summary

The Black Island area is located at the boundary between a ca. 3.0 Ga craton, the North Caribou Terrane, and the Neoarchean volcanic rocks of the Uchi Subprovince. This boundary is rarely well preserved to the east of the Black Island area, so the excellent exposures on Lake Winnipeg provide unique insight into the 3.0 Ga craton, an unconformable 2.98 Ga rift sequence, a 2.72 Ga oceanic volcanic package, two 2.71 Ga sedimentary-overlap sequences and the nature of contacts among these domains.

On the basis of widespread platform sedimentary-cover sequences, exposed in Ontario, the North Caribou Terrane has been interpreted to represent a stable crustal setting by ca. 3.0 Ga (Thurston et al., 1991). The 2.98 Ga Lewis-Storey rift sequence on ca. 3.0 Ga basement at Lake Winnipeg suggests that this crustal stability was short lived and the opening of an ocean basin to the west. Possible correlatives to the Lewis-Storey assemblage are exposed along the southern flank of the North Caribou Terrane to the east, in the Wallace Lake and Red Lake greenstone belts (Figure 1). The geological history of the southern flank of the North Caribou Terrane, however, differs substantially from that at the southwestern margin at Lake Winnipeg. For instance, at Red Lake, the Balmer assemblage was overlain by 2.94, 2.92, 2.89, 2.85 and 2.75–2.73 Ga arc-like sequences prior to Uchian tectonism at ca. 2.71–2.70 Ga (Sanborn-Barrie et al., 2001, 2004). In contrast, the >2.978 Ga Lewis-Storey rift assemblage at Lake Winnipeg appears to mark the beginning of a 260 m.y. depositional hiatus at the southwestern edge of the craton.

The Black Island oceanic assemblage represents a terrane without stratigraphic or geochemical affinity to the North Caribou Terrane. The lower Gray Point volcanic sequence is an

isotopically juvenile ocean-floor-back-arc sequence. The internal discontinuity between the Gray Point and Drumming Point sequences marks an apparent change from ocean-floor-back-arc to arc magmatism and may reflect a plate reorganization event. Negative  $\epsilon_{Nd}$  values for the Drumming Point volcanic rocks suggest possible contamination by older crust, through either subduction-zone enrichment or construction on continental basement.

Juxtaposition of the Black Island oceanic assemblage with the North Caribou margin occurred on northwest-trending, transcurrent  $D_1$  structures, probably around 2.71 Ga. The oblique nature of docking at this margin may account for the generally excellent preservation state of primary features, as well as formation of local depocentres attracting coarse clastic sediments. Subsequent  $D_2$  and  $D_3$  structures in all supracrustal units likely represent progressive strain increments (cf. Anderson, 2003) accompanying the 2.71–2.70 Ga collisional Uchian orogeny.

Similar to areas to the east at Bissett and Red Lake, the Black Island area has considerable potential for lode-gold mineralization. The context for this mineralization has been enhanced by the new mapping and improved structural understanding of the area. The rift-margin Lewis-Storey sequence has exploration potential for Ni and PGE. The diamond potential of the Black Island area and in the ancient North Caribou Terrane to the northeast has not been assessed. A possible arc-rifting event at the top of the Gray Point sequence on Lake Winnipeg and VMS-style alteration and sulphide fragments in volcanoclastic rocks near the top of the Bidou subgroup east of Bissett (Anderson, 2004) indicate that the Rice Lake greenstone belt may have potential to host base-metal mineralization.

## Acknowledgments

This report summarizes results from a project that was jointly undertaken by the Manitoba Geological Survey and the Geological Survey of Canada. It is a product of the GSC-sponsored Western Superior NATMAP project (contribution number 2005159).

Field assistance during the 2000 mapping program was provided by Mike Surka and Jean-Francois Ravenelle. Doug Berk and the staff of the Rock Preparation Laboratory (MGS) provided logistical support in the field and preparation of rock samples for geochemical analysis. Maps accompanying this

report were ably drafted by Maureen McFarlane (MGS). The figures were prepared by Bonnie Lenton (MGS). V. McNicoll (GSC) assisted with collection of the geochronological samples and undertook their subsequent analysis and interpretation. K. Tomlinson (GSC) provided much-needed supervision of the isotopic analytical work and subsequent processing of the data. The report benefited from a constructive and careful scientific edit by Neil Rodgers (GSC) and a thorough technical edit by Bob Davie (RnD Technical).

## References

- Anderson, S.D. 2003: Geology and structure of the Garner Lake area, southeast Rice Lake greenstone belt, Manitoba (NTS 52L14); *in* Report of Activities 2003, Manitoba Industry, Economic Development and Mines, Manitoba Geological Survey, p. 178–195.
- Anderson, S.D. 2004: Preliminary results and economic significance of geological mapping and structural analysis in the Rice Lake area, central Rice Lake greenstone belt, Manitoba (NTS 52M4 and 52L13); *in* Report of Activities 2004, Manitoba Industry, Economic Development and Mines, Manitoba Geological Survey, p. 216–231.
- Bailes, A.H. and Percival, J.A. 2000: Geology and structure of the North Caribou Terrane–Uchi Subprovince boundary in eastern Manitoba with emphasis on volcanic and volcanoclastic rocks of the Black Island assemblage, Manitoba; *in* Report of Activities 2000, Manitoba Industry, Trade and Mines, Manitoba Geological Survey, p. 161–174.
- Bailes, A.H., Percival, J.A., Corkery, M.T., McNicoll, V.J., Tomlinson, K.Y., Rogers, N., Sasseville, C., Whalen, J.B. and Stone, D. 2003: Geology and tectonostratigraphic assemblages, west Uchi map area, Manitoba/Ontario; Manitoba Industry, Trade and Mines, Manitoba Geological Survey, Open File Report OF2003-1, 1 full colour map, scale 1:250 000.
- Barrett, T.J. and MacLean, W.H. 1994: Chemostratigraphy and hydrothermal alteration in exploration for VHMS deposits in greenstones and younger volcanic rocks; *in* Alteration and Alteration Processes Associated with Ore-Forming Systems, D.R. Lentz (ed.), Geological Association of Canada, Short Course Notes, Volume II, p. 433–465.
- Brown, A. 1981: Geology, Black Island, Lake Winnipeg, Manitoba; Geological Survey of Canada, Open File 812, 9 maps, scale 1:15 840.
- Corfu, F. and Stone, D. 1998: Age, structure and orogenic significance of the Berens River composite batholiths, western Superior Province; Canadian Journal of Earth Sciences, v. 35, p. 1089–1109.
- Currie, M. 2001: Greenschist facies metamorphism of 2.72 Ga juvenile metabasites of westernmost Uchi subprovince, Manitoba, Canada; B.Sc. thesis, Carleton University, Ottawa, Ontario.
- Davies, J.F. 1951: Geology of the Manigotagan–Rice River area; Manitoba Department of Mines and Natural Resources; Mines Branch, Publication 50-2, 16 p.
- DePaolo, D.J. 1988: Age dependence of the composition of continental crust: evidence from Nd isotopic variations in granitic rocks; Earth and Planetary Science Letters, v. 90, no. 3, p. 263–271.
- Ermanovics, I.F. 1970: Precambrian geology of the Hecla–Carroll Lake map area, Manitoba-Ontario (62P E1/2, 52M W1/2); Geological Survey of Canada, Paper 69-42, 33 p.
- Ermanovics, I.F. 1981: Geology of the Manigotagan area, Manitoba; Geological Survey of Canada, Paper 80-26, 14 p.
- Ermanovics, I.F. and Wanless, R.K. 1983: Isotopic age studies and tectonic interpretation of Superior Province in Manitoba; Geological Survey of Canada, Paper 82-12, 17 p.
- Gribble, R.F., Stern, R.J., Bloomer, S.H., Stuben, D., O’Hearne, T. and Newman, S. 1996: MORB mantle and subduction components interact to generate basalts in the southern Mariana Trough back-arc basin; Geochimica et Cosmochimica Acta, v. 60, no. 12, p. 2153–2166.
- Jensen, L.S. 1976: A new cation plot for classifying subalkaline volcanic rocks; Ontario Division of Mines, Miscellaneous Paper 66, 22 p.
- Krogh, T.E., Ermanovics, I.F. and Davis, G.L. 1974: Two episodes of metamorphism and deformation in the Archean rocks of the Canadian Shield; Carnegie Institution of Washington, Geophysical Laboratory Yearbook, p. 573–575.
- LeMaitre, R.W., Bateman, P., Dudek, A., Keller, J., Lameyre, J., LeBas, M.J., Sabine, P.A., Schmid, R., Sorensen, H., Wooley, A.R. and Zanettin, B. 1989: A Classification of Igneous Rocks and Glossary of Terms; Blackwell Scientific Publications, Oxford, United Kingdom, 193 p.
- Mamberti, M., Lapierre, H., Bosch, D., Jaillard, E., Hernandez, J. and Polvé, J. 2004: The Early Cretaceous San Juan Plutonic Suite, Ecuador: a magma chamber in an oceanic plateau? Canadian Journal of Earth Sciences, v. 42, p. 1237–1258.

- Marr, J.M. 1971: Petrology of the Wanipigow River suite, Manitoba; *in* Geology and Geophysics of the Rice Lake Region, Southeastern Manitoba (Project Pioneer), W.D. McRitchie and W. Weber (ed.), Manitoba Department of Mines, Resources and Environmental Management, Mines Branch, Publication 71-1, p. 203–214.
- Pearce, J.A. 1975: Basalt geochemistry used to investigate past tectonic environments on Cyprus; *Tectonophysics*, v. 25, p. 41–67.
- Pearce, J.A. 1983: Role of subcontinental lithosphere in magma genesis at active continental margins; *in* Continental Basalts and Mantle Xenoliths, C.J. Hawkesworth and M.J. Norry, Shiva Publications, Nantwich, United Kingdom, p. 230–249.
- Pearce, J.A. 1996: A user's guide to basalt discrimination diagrams; *in* Trace Element Geochemistry of Volcanic Rocks: Applications for Massive Sulphide Exploration, D.A. Wyman (ed.), Geological Association of Canada, Short Course Notes, v. 12, p. 79–113.
- Pearce, J.A. and Cann, J.R. 1973: Tectonic setting of basic volcanic rocks determined using trace element analysis; *Earth and Planetary Science Letters*, v. 19, p. 290–300.
- Pearce, J.A. and Peate, D.W. 1995: Tectonic implications of the composition of volcanic arc magma; *Annual Review of Earth and Planetary Sciences*, v. 23, p. 251–285.
- Pearce, J.A., Harris, N.B.W. and Tindle, A.G. 1984: Trace element discrimination plots for the tectonic interpretation of granitic rocks; *Journal of Petrology*, v. 25, p. 956–983.
- Percival, J.A. and Whalen, J.B. 2000: Observations on the North Caribou terrane–Uchi Subprovince interface in western Ontario and eastern Manitoba; *Geological Survey of Canada, Current Research*, 2000-C15, 8 p.
- Percival, J.A., Bailes, A.H. and McNicoll, V. 2001: Mesoarchean western margin of the Superior Craton in the Lake Winnipeg area, Manitoba; *Geological Survey of Canada, Current Research* 2002-C16, 19 p.
- Percival, J.A., Bailes, A.H. and McNicoll, V. 2002: Mesoarchean breakup, Neoarchean accretion, in the western Superior Craton, Lake Winnipeg, Manitoba, Canada; *Geological Association of Canada–Mineralogical Association of Canada, Joint Annual Meeting*, Saskatoon, Saskatchewan, May 27–29, 2002, Field Trip B3 Guidebook, 42 p.
- Percival, J.A., Whalen, J.B. and McNicoll, V. 2000: Tectonic reconstruction of the western Uchi Subprovince; *in* Western Superior Transect Sixth Annual Workshop, R.M. Harrap and H. Helmstaedt (ed.), LITHOPROBE Secretariat, University of British Columbia, LITHOPROBE Report 77, p. A2–A4.
- Poulsen, K.H., Weber, W., Brommecker, R. and Seneshen, D.N. 1996: Lithostratigraphic assembly and structural setting of gold mineralization in the eastern Rice Lake greenstone belt, Manitoba; *Geological Association of Canada–Mineralogical Association of Canada, Joint Annual Meeting*, Field Trip A4 Guidebook, 106 p.
- Rainbird, R.H. and Ernst, R.E. 2001: The sedimentary record of mantle plume uplift; *in* Mantle Plumes: Their Identification Through Time, R.E. Ernst and K.L. Buchan (ed.), Geological Society of America, Special Paper 352, p. 227–246.
- Ravenelle, J.F. 2001: Geochemistry of an ultramafic megabreccia, English Lake complex, Manitoba; B.Sc. thesis, McGill University, Montreal.
- Richardson, S.H., Gurney, J.J., Erlank, A.J. and Harris, J.W. 1984: Origin of diamonds in old enriched mantle; *Nature*, v. 310, p. 198–202.
- Sanborn-Barrie, M., Rogers, N., Skulski, T., Parker, J.R., McNicoll, V. and Devaney, J. 2004: Geology and tectonostratigraphic assemblages, east Uchi, Red Lake and Birch-Uchi belts, Ontario; *Geological Survey of Canada, Open File* 4256; Ontario Geological Survey, Preliminary Map P.3460, scale 1:250 000.
- Sanborn-Barrie, M., Skulski, T. and Parker, J.R. 2001: Three hundred million years of tectonic history recorded by the Red Lake greenstone belt, Ontario; *Geological Survey of Canada, Current Research* 2001-C19, 19 p.
- Sasseville, C. and Tomlinson, K.Y. 2000: Structure and stratigraphy of the Mesoarchean Wallace Lake greenstone belt, southeastern Manitoba; *Geological Survey of Canada, Current Research* 2000-C15, 8 p.
- Saunders, A.D., Norry, M.J. and Tarney, J. 1991: Fluid influence on the trace element compositions of subduction zone magmas; *Philosophical Transactions: Physical Sciences and Engineering*, v. 335, no. 1638, p. 377–392.
- Sinton, J.M. and Fryer, P. 1987: Mariana Trough lavas from 18°N: implications for the origin of back arc basin basalts; *Journal of Geophysical Research*, v. 92, no. B12, p. 12782–12802.
- Stern, R.A., Syme, E.C. and Lucas, S.B. 1995: Geochemistry of 1.9 Ga MORB- and OIB-like basalts from the Amisk collage, Flin Flon belt, Canada: evidence for an intra-oceanic origin; *Geochimica et Cosmochimica Acta*, v. 59, p. 3131–3154.
- Stolper, E.W. and Newman, S. 1994: The role of water in the petrogenesis of Mariana Trough magmas; *Earth and Planetary Science Letters*, v. 121, no. 3–4, p. 293–325.
- Stone, D. 1998: Precambrian geology of the Berens River area, northwest Ontario; *Ontario Geological Survey, Open File Report* 5963, 115 p.
- Sun, S.S. and McDonough, W.F. 1989: Chemical and isotopic systematics of oceanic basalts: implications for mantle composition and processes; *Geological Society, Special Publications*, v. 42, p. 313–345.
- Swinden, H.S. 1996: The application of volcanic geochemistry to the metallogeny of volcanic-hosted sulphide deposits in central Newfoundland; *in* Trace Element Geochemistry of Volcanic Rocks: Applications for Massive Sulphide Exploration, D.A. Wyman (ed.), Geological Association of Canada, Short Course Notes, v. 12, p. 329–358.

- Syme, E.C. 1998: Ore-associated and barren rhyolites in the central Flin Flon belt: case study of the Flin Flon mine sequence; Manitoba Energy and Mines, Geological Services, Open File Report OF98-9, 26 p.
- Thurston, P.C., Osmani, I.A. and Stone, D. 1991: Northwestern Superior Province: review and terrane analysis; *in* Geology of Ontario, P.C. Thurston, H.R. Williams, R.H. Sutcliffe and G.M. Stott (ed.), Ontario Geological Survey, Special Volume 4, Pt. 1, p. 81–144.
- Turek, A. and Weber, W. 1994: The 3 Ga granitoid basement to the Rice Lake supracrustal rocks, southeast Manitoba; *in* Report of Activities, 1994, Manitoba Energy and Mines, Geological Services, p. 167–169.
- Turek, A., Keller, R., Van Schmus, W.R. and Weber, W. 1989: U-Pb zircon ages for the Rice Lake area, southeastern Manitoba; Canadian Journal of Earth Sciences, v. 26, p. 23–30.
- Whalen, J.B., Percival, J.A., McNicoll, V. and Longstaffe, F.J. 2003: Intra-oceanic production of continental crust in a Th-depleted ca. 3.0 Ga arc complex, western Superior Province, Canada; Contributions to Mineralogy and Petrology, v. 146, no. 1, p. 78–99.
- Winchester, J.A. and Floyd, P.A. 1977: Geochemical discrimination of different magma series and their differentiation products using immobile elements; Chemical Geology, v. 20, p. 325–343.
- Wood, D.A. 1980: The application of Th-Hf-Ta plots to problems of tectonomagmatic classification and to establishing the nature of crustal contamination of basaltic lavas of the British Tertiary Volcanic Province; Earth and Planetary Science Letters, v. 50, p. 11–30.
- Young, J. and Theyer, P. 1990: Geology of mafic-ultramafic intrusive rocks in the English Lake area (NTS 62P/1); *in* Report of Activities, 1990, Manitoba Energy and Mines, Minerals Division, p. 111–113.